The University of Sydney
Australia

"Design of an Autonomous Hovering Miniature Air Vehicle as a Flying Research Platform"

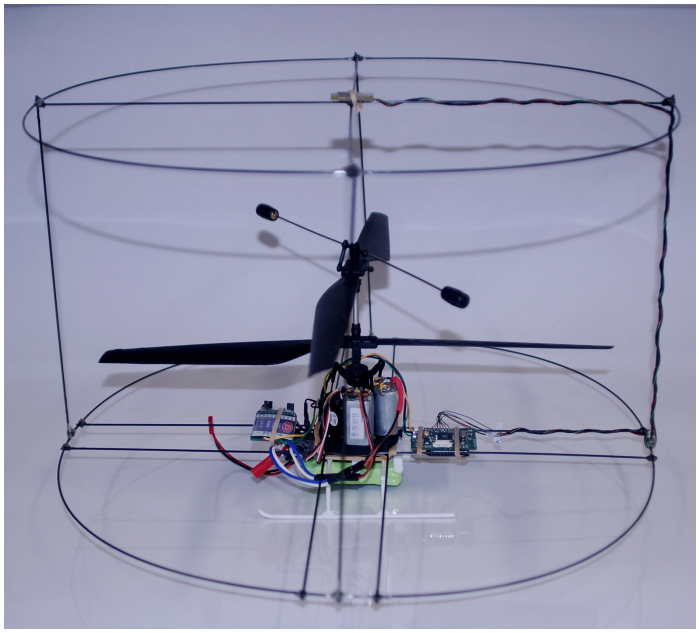

By

James F. Roberts, B.E (Microelectronic Eng.)

Submitted in fulfilment of the requirements for the degree of Master of Engineering Research

The University of Sydney

New South Wales
Australia

March, 2007

Project Contact Details:

MER Student:

Name: James F. Roberts – University of Sydney
Address: Silky Ridge, 104 Stokers Rd
Stokers Siding, NSW, 2484
Phone: +61-2-66-779530
Fax: +61-2-66-779100
Email: **james.roberts@jimonics.com**

Project Supervisor:

Name: Dr KC Wong – University of Sydney
Address: Room N312
J11 - Aeronautical Engineering Building
University of Sydney
NSW 2006 Australia
Phone: +61 4 1348 2519
Fax: +61 2 9351 4841
E-mail: **kc@aeromech.usyd.edu.au**

Associate Supervisor:

Name: Dr Doug Auld – University of Sydney
Address: Room N310
J11 - Aeronautical Engineering Building
University of Sydney
NSW 2006 Australia
Phone: +61 2 9351 2336
Fax: +61 2 9351 4841
E-mail: **d.auld@usyd.edu.au**

Table of Contents:

List of Equations:

List of Figures:

I. Acknowledgments

I. Acknowledgments:

I would like to take this opportunity to thank the people who were involved in the project. I am grateful for all the help and support they gave me throughout my research. I especially want to thank the following people:

- Dr KC Wong for his knowledgeable input into the project and aeronautical expertise in MAV design. KC's interest in microelectronics together with his open minded approach allowed me to come up with innovative designs that were not bounded by classical design approaches. KC helped me bridge the gap between aeronautical and microelectronic engineering, enabling me to develop a successful prototype autonomous hovering system.

- Dr Doug Auld & Dr Hugh Stone for being interested in my area of research and I am grateful of their input. Their ideas about how to approach various problems that arose throughout the project and their experience and theoretical knowledge in UAV's was very useful. It was especially educational (and good fun) to get out in the field and be a part of the experimental flight testing of Hugh Stone's Vertical take off and landing 'T-wing' UAV.

- Kristine and Raymond Roberts for their unconditional love and backing, both financially and emotionally, throughout the course of my post graduate studies. I truly could not have done so much without their support.

- Kevin Roberts for the weekly ‘meetings’. They were both inspiring and delicious. The fine dining and great selection of New Zealand wines were an experience that I will never forget.

- My Fellow Colleagues, in particularly; Alex, Volker and the ‘Jabirologists’ down stairs for being my great mates. They made going to the USYD something fun and something to look forward to each day.

II. Statement of Originality

II. Statement of Originality:

The material presented in this report contains all of my own work. To the best of my knowledge and belief, this thesis contains no material previously published or written by another person except where due acknowledgment is made in the report itself.

MER STUDENT

Name: James F. Roberts

Signed: 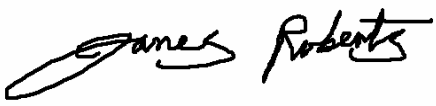

Dated: March 25, 2007

III. Executive Summary

III. Executive Summary:

This thesis, by developing a Miniature Aerial Vehicle (MAV) hovering platform, presents a practical solution to allow researchers and students to implement their theoretical methods for guidance and navigation in the real world. The thesis is not concerned with the development of guidance and navigation algorithms, nor is it concerned with the development of external sensors.

There have been some recent advances in guidance and navigation towards developing algorithms and simple sensors for MAVs. The task of developing a platform to test such advancements is the subject of this thesis. It is considered a difficult and time consuming process due to the complexities of autonomous flight control and the strict size, weight and computational requirements of this type of system.

It would be highly beneficial to be able to buy a platform specifically designed for this task that already possesses autonomous hovering capability and the expansion connectivity for interfacing your own custom developed sensors and algorithms. Many biological and computer scientists would jump at the opportunity to maximize their research by real world implementation.

The development of such a system is not a trivial task. It requires a great deal of understanding in a broad range of fields including; Aeronautical, Microelectronic, Mechanical, Computer and Embedded Software Engineering in order to create a successful prototype.

The challenge of this thesis was to design a research platform to enable easy implementation of external sensors and guidance algorithms, in a real world environment for research and education. The system is designed so it could be used for a broad range of testing experiments.

After extensive research in current MAV and avionics design it became obvious in several areas the best available products were not sufficient to meet the needs of the proposed platform. Therefore it was necessary to custom design and build; sensors, a data acquisition system and a servo controller. The latter two products are available for sale by Jimonics [1]. It was then necessary to develop a complete flight control system with integrated sensors, processor and wireless communications network which is called 'The MicroBrain'. 'The MicroBrain' board measures only 45mm x 35mm x 11mm and weighs ~11 grams. The coaxial contra-rotating MAV platform design provides a high level of mechanical stability to help minimise the control system complexity. The platform was highly modified from a commercially available remotely controlled helicopter. The system incorporates a novel collision protection system that was designed to also double as a mounting place for external sensors around its perimeter.

The platform equipped with 'The MicroBrain' is capable of fully autonomous hover. This provides a great base for testing guidance and navigational sensors and algorithms by decoupling the difficult task of platform design and low-level stability control.

By developing a platform with these capabilities the researcher can now focus on the guidance and navigation task, as the difficulties in developing a custom platform have been taken care of. This therefore promotes a faster evolution of guidance and navigational control algorithms for MAVs.

VIDEO NOTE: The videos mentioned throughout the thesis can be found attached to the back binding in compact disc form. An example of the naming convention used in the thesis is:

(See "Onboard Camera" video)

This refers to the video file named ***"1.0 Onboard Camera.avi"*** *where the preceding numbers refer to the actual heading number. This would be found under the folder with the corresponding chapter label e.g.* ***"Chapter 1"****. For those who are reading a soft copy feel free to contact the author to arrange to view the videos.*

Chapter 1

1.0 Introduction:

The first aerial robot was developed in 1863 during the American Civil War. The simple design consisted of a hot air balloon equipped with a basket of explosives. A timer activated a hinge on the basket below dropping the ignited explosives on the enemy [2]. Since then there have been huge advancements in aerial robotic technologies. The availability of advanced; materials, propulsion systems, Micro-Electro-Mechanical Systems (MEMS) sensors, high speed microcontrollers etc. have opened the way for some innovative and interesting applications. Today a large portion of research is going into developing Miniature Aerial Vehicle (MAV) platforms and control systems to achieve more complex missions. Hovering MAV platforms are particularly interesting as they are capable of flying in cluttered indoor environments. The question is why you would want to fly in such situations? With an increasing number of terrorist attacks and environmental disasters there are more and more reasons for entering structurally un-safe buildings to do search and rescue missions. Ground based robots have been useful in the past but have shown their limitations in mobility due to the harsh environment in which they are required to manoeuvre. A flying robot could provide a more manoeuvrable and efficient solution. A simple application could be a remotely controlled self stabilizing hovering platform fitted with a wireless camera. This would allow the rescuer to extend their vision thus enabling them to find trapped or injured persons within a target building. (***See "Onboard Camera" video***) This is within the grasp of this thesis project and has the potential to 'save lives'.

This could be taken one step further by replacing the human operator altogether. In order to do this the robot would need some form of guidance and navigation, and also be able to detect victims. Body heat could be a good measure for finding a victim in such situations however this is out of the scope of this project. Navigating indoors is an extremely difficult task for an MAV to accomplish with no reference or co-ordinate system available. Traditional GPS based navigation systems cannot be used as GPS is not reliable in such environments.

To attempt to solve this problem some scientists are looking towards nature for inspiration, for example of this is the current research on the honey bee [3]. Honey bees are capable of flying long distances and are able to hover. They are able to navigate from their hive to a flower, collect pollen, and then navigate back to their hive in a relatively efficient manner. This is much like the search and rescue mission above. How does the honey bee accomplish this with a brain that has a similar processing capability as a high-end microcontroller?

Scientists have been studying insects in order to understand how to develop guidance and navigation algorithms and simple sensors (such as optical flow) that could be used on MAV platforms [3]. The task of developing the actual platform to test such advancements is often out of reach for the typical biological or computer scientist. It requires a broad range of expert knowledge in the fields of; Aeronautical, Microelectronic, Mechanical, Computer Software and Embedded Software Engineering.

This project is aimed at designing and constructing an indoor hovering MAV with autonomous low-level stability control. The platform will have the ability to add external experimental sensors making it useful for testing higher level sensors and algorithms. The system design uses the minimum sensor and processing requirements for full autonomy thus increasing the available payload and processing power for these additional external sensors.

There are a number of foreseen problems that will require extensive research before the system prototype can be realised. These problems can be raised with a set of specific questions as seen below:

- What is the state of the art in MAV technologies including; materials, propulsion system, sensors and avionics?
- What kind of platform is the most suitable for the project?
- What are the limitations of this platform in regard to stability, controllability and available payload?
- What is the minimum sensor requirement for the chosen platform and how are they going to be tested and integrated?
- How are the external sensors going to be mounted?

- Does a microcontroller have enough processing capability for full autonomous control?

- Is it possible to integrate all this on a single printed circuit board (PCB) for miniaturisation, elegance and simplicity?

- How do you test such a system safely and still achieve a rapid development time?

Extensive research has been done to find the answers to these questions. Currently it is believed that there are no complete fully autonomous hovering MAV systems with this kind of flexibility, which are designed to support experimental testing with minimal effort.

1.1 System Requirements:

First a definition of the system requirements will be made which are critical in the pursuit of a successful hovering platform design that matches the desired application. Below is a discussion on the most important requirements that will steer the research and determine how the platform is developed:

1.1.1 Platform:

The platform must be lightweight and small. There is a balance between the size of the platform and how much it can carry as payload. A larger platform can carry more weight however it must be suited to the environment in which it will be used. As this system is designed for indoors it is desirable to fit through standard door openings (~700mm) with some clearance on either side. Therefore the chosen maximum diameter of platform is 400mm.

The system must be user friendly to allow for easy implementation to the desired application. If the system is easy to use and robust then it will be accepted by a larger research group and naturally start to promote itself into the market place. Robustness is important as the environment in which the system operates is of a high impact nature. The walls, floor and ceiling suddenly become potentially dangerous when flying indoors. Therefore it is necessary to design a system that can withstand small collisions and allow the system to "bounce" off potentially dangerous obstacles without damaging the platform.

Indoor flight presents an environment that is naturally cluttered with tight corners and narrow hall ways. Thus a platform with a high degree of manoeuvrability and the ability to hover would be most desirable. Lighter than air vehicles (LTAV) [4] are easy to implement due to the slow dynamics created by the buoyancy and air resistance, however, this dampens their manoeuvrability and controllability making them slow and docile.

Also the system would require a large volume of Helium in order to carry all the required avionics and payload. Flapping wing technology has come a long way in the recent years, designs are now capable of high manoeuvrability, hovering, and vertical take-off and landing [5], however, they are fragile and have a very limited payload capability, in the order of grams for an indoor system, they are also very difficult to control. Conventional helicopters are difficult to control due to their inherent instabilities. These systems usually require; precise sensors, a fast processing capability and some sort of global positioning system. This is a real challenge for a platform of this size and weight. A better solution would be to use an inherently stable platform that utilises a degree of mechanical stability.

To be useful for flying experiments it is necessary to have an endurance that is long enough to view how the system behaves and responds to the environment in which it is flying. An endurance of ~10min would be a realistic amount of time to study how the sensors and algorithms respond and to allow for numerous unknown situations to arise.

There are an endless number of external sensors that could be implemented on the system. This makes it extremely difficult to have an optimal mounting place for every type of sensor available. Therefore is it necessary to have a generic mounting system that can provide a full 360° mounting area to allow for flexibility when attaching external sensors. This gives the experimenter the ability to place the external sensors exactly where they are required with minimal effort.

The payload directly affects the endurance of the platform. This payload capacity has been calculated based on a 25% body weight for a flight time of ~10min. This can be concluded after numerous manual flight tests.

A summary of the platform requirements can be seen below:

- Be lightweight (~200g) and small (~400mm)
- Be easy to use and robust
- Able to withstand small collisions
- Have hovering capabilities
- Be maximally inherently stable
- High manoeuvrability inside a cluttered environment
- Have a respectable endurance (~10min with maximum payload)
- Have a 360° mounting area for external sensors
- Have a respectable payload capacity for external sensors (~50g)

1.1.2 Control and sensors:

The system will need to be able to decouple the difficulty of autonomous low-level flight control and simplify the control into a set of standard commands e.g. forward, backward, left, right, rotate left, rotate right, upward and downward. In order to accomplish this appropriate low-level sensors and controllers need to be selected carefully.

The external sensors will need to be provided with power and general connectivity to the platforms avionics. This connectivity is the actual interface for autonomously controlling and commanding the platform. The power supplied should be of a nominal voltage that can be stepped down on the sensor boards to lower voltages as required.

The system will need a communications link to allow for manual control, autonomous activation/deactivation and data logging from the sensors and controllers. Therefore a two-way link is required that has a reasonable bandwidth and consumes minimal power. A communications system with a networking capability would be desirable to allow for numerous platforms to communicate. This could provide communications for higher level collaboration such as swarming algorithms.

A sub-autonomous mode where the system self-stabilises and can be controlled remotely by a pilot with minimal experience would be a goal system test. This is an easy way to show how the system performs without having to add the external sensors.

A summary of the control and sensor requirements can be seen below:

- Low-level flight control (attitude, heading, and altitude)
- Allow for external sensor connectivity including power
- Have an up link for manual radio control
- Have a down link for acquiring sensor and system data
- Capability to be controlled remotely by an operator with minimal experience

The system design can be broken up into three major sections; platform design, avionics hardware design and avionics software design. Each of these sections will provide the details of the final design and the process in which they were created. After the system design sections the operational testing stage will be discussed to evaluate the performance of the final system. The tests will then be collectively discussed and evaluated to give an overview of the goals achieved from the initial specifications. Most of the tests have been documented on camera and have been attached to the back of the thesis in compact disc form.

1.2 Research and Education

Currently there are no known indoor hovering platforms available which possess the requirements as stated above. However, there are several ground based robots available that are designed for research and education. Here we will briefly discuss two of these systems, the e-puck and the Khepera III, chosen for their small size and good reputation.

The e-puck [6] is a miniature mobile robot designed to be an educational tool for robotics research at a university level. Powered by a dsPIC core the hockey puck sized robot has a variety of different sensors including three microphones, three-axis accelerometer, eight proximity detectors and a VGA camera. The modular design allows additional turrets to be connected including omni-directional vision, fly vision, ground sensors and magnetic wheels. The e-puck has proven to be a cheap, robust and useful tool enabling researchers and students to perform practical experiments.

The Khepera III [7] is a slightly larger mobile robot designed to be an educational tool for robotic experimentation at a university level. Also powered by a dsPIC core the 130mm diameter robot has a variety of different sensors including nine infrared proximity and ambient light sensors, two infrared ground proximity sensors for line following applications and five long range ultrasonic distance sensors. The design allows for additional modules to be connected including a Linux computer, sound processing, gripper and wireless communication. The Khepera range of robots has proven to be a high quality, robust and useful tool enabling researchers and students to perform experiments such as navigation, artificial intelligence, multi-agents systems, control and real-time programming.

It is obvious that developments with ground based robotics for research and education is well matured, however, developments with indoor flying robotics are still very young. The toy industry has recently accelerated this field towards robust and cheap radio controlled helicopters. However, there are still no indoor flying robots for research and education commercially available. In order to accelerate the use of autonomous robotics in such systems it may be interesting to learn some lessons from the matured ground based systems. Such key features may include robustness, simplicity in design, ease-of-use, modularity, and external connectivity.

Chapter 2

2.0 Platform Research:

A range of MAV platforms which have indoor hovering capabilities, both commercial and experimental will be reviewed. Each design will be evaluated in the trade off between stability and controllability. A closer look at some of the latest developments in control mechanisms will be undertaken to find a suitable design solution.

2.1 Commercially Available Platforms:

Here we will take a look at three designs introduced by the toy industry the; Proxflyer – Blade Runner, X-UFO and the Twister Bell-47. We will evaluate each of their performances and determine their suitability for the project:

Figure 1: Proxflyer - Blade Runner [8]

The Proxflyer, developed by Peter Murren [8] (see figure 1), has traded-off greater stability for a decrease in manoeuvrability. Its complexity is relatively high due to the semi-articulated hub assembly and four bladed rotor designs (see figure 2). It is a very stable design which ingeniously allows the rotors to tilt up, thus creating a horizontal force which dampens the induced motion before it can take affect. The four semi-

articulated blades are hinged only to allow upward and downward motion. No known analysis of this system has been published to determine exactly how this works. Indoors this design produces very little drift even without any kind of electronic feedback.

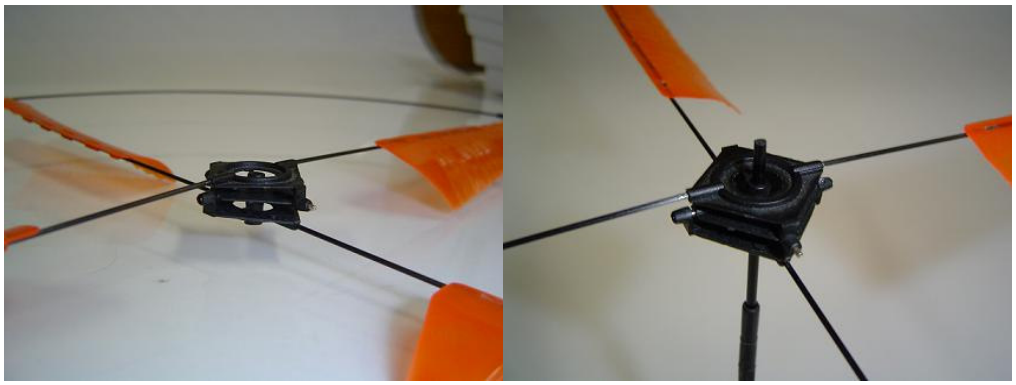

Figure 2: Proxflyer Semi-articulated Blades [9]

The downfall of this design is that it has a very limited horizontal speed. Forward movement is achieved by thrusters which slightly angle the top rotor thus moving the platform forward. This makes the design un-suitable for outdoor flying, as there is not enough control authority to compensate for even the smallest disturbance.

Figure 3: X-UFO quad rotor [10]

The X-UFO quad rotor (see figure 3) has traded-off more controllability for a decrease in stability. Its hardware complexity is relatively low due to the simple design, thus making

it very easy to build. The platform has a relatively good lifting capacity, and due to its high controllability, it can fly in reasonably strong winds. The downfall of this design is that it requires either high-speed control techniques or non-linear controllers to stabilise the system. Complicated sensing and data fusion would also be required for fully autonomous control.

Figure 4: Twister Bell-47 [11]

The Twister Bell-47 (see figure 4) design is not as stable as the Proxflyer but takes the middle ground between stability and manoeuvrability. Its hardware complexity is relatively high due to the semi-articulation and cyclic designs (see figure 5) [12]. It is a stable, two bladed design which uses a gyroscopic bar to force the top rotor to stay, while the body rocks and absorbs the disturbance underneath. This is achieved by a semi-articulated hinge which allows rotation of the pitch only. The bottom rotor has no stabilisation except for gyroscopic and is purely designed for cyclic control. By altering the angle of the swash plate, the pitch of the rotor is periodically altered thus allowing translation in the reactive direction.

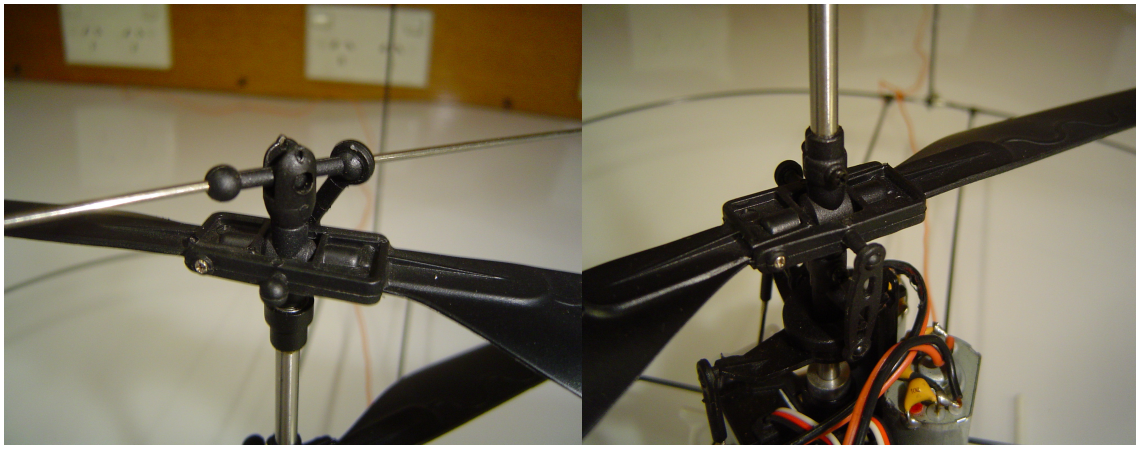

Figure 5: Left - Top rotor semi-articulated stabiliser, Right - Bottom rotor cyclic [13]

The top stabilizer bar is placed at 45˚ advancing the rotor and the cyclic inputs are at -45˚ this adds to the 90˚ action vs. reaction of the precession effect (see figure 6).

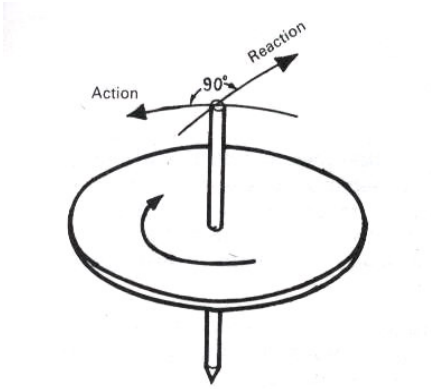

Figure 6: Precession effect [14]

2.2 Other Research Platforms:

The Coander Effect MAV (see figure 7) is a new design that uses a single propulsion unit situated on the top of the platform. It is a design with medium complexity and relatively good controllability (as seen in test videos [15]). A duct around this motor directs the airflow across the top surface and increases the efficiency. The Coander Effect results in

the airflow hugging the top surface curvature. It generates thrust by decreasing the air pressure around the top surface of the platform thus resulting in a lifting force. The yaw is controlled using numerous "D" shaped control vanes which rotate left or right to compensate for the reactive torque generated by the motor. Control vanes around the bottom perimeter allow the platform to translate in any direction. The platform is somewhat neutrally stable, but requires a lot of thrust to work due to the indirect airflow and weight of the structure [16]. The platform is currently remote controlled. However the designers are working on a much larger prototype (due to the limited excess thrust) able to carry the avionics required for autonomy.

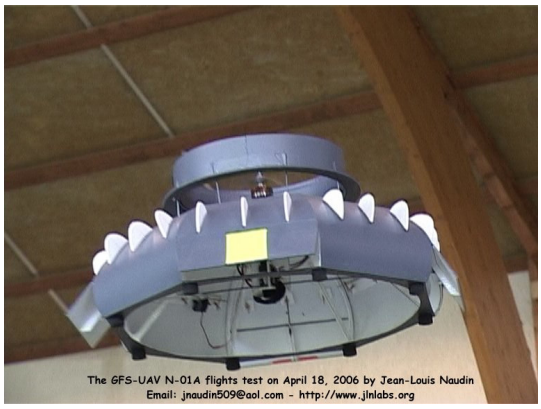

Figure 7: Coander effect MAV [15]

The iStar MAV (see figure 8) [17] is a design that uses a single gas engine directly fixed to a propeller surrounded by an aerodynamic duct. Control is achieved using control vanes around the exit of the duct. The iStar is believed to be the first hovering MAV to translate from vertical to horizontal flight (made possible by the aerodynamic duct). The iStar design has a medium hardware complexity and is relatively unstable requiring inertial sensors to allow for remote controlled flight.

Figure 8: iStar MAV [17]

The MicroDrone MAV (see figure 9) [18] is a design similar in concept to the X-UFO. It has four brushless motors and is equipped with a fully autonomous flight computer including: attitude, altitude and GPS control systems. The platform can fly fully autonomous with no human intervention. Its main development application is for outdoor aerial surveillance. Everything on the platform has been custom designed even the brushless motors. The same pros and cons for the X-UFO apply to this platform. The platform uses GPS to correct for position drift and has no platform self preservation devices, therefore it is not suited for indoor operations without some modifications. None-the-less its outdoor performance is outstanding (The test videos of this platform are impressive [19]).

Figure 9: MicroDrone MD4-200 [19]

The Drexel Hovering Fixed Wing MAV (see figure 10) [20] is a design that uses a standard foam fixed wing plane, in the vertical configuration. It is relatively simple in design but it requires accurate inertial sensors and computationally expensive controllers to fly in hovering mode. The platform has sustained an autonomous hover for up to 90 seconds. In the horizontal configuration the platform would provide good endurance. However as an indoor experimentation platform it would be necessary to be able to hover continuously, therefore this design is definitely not viable.

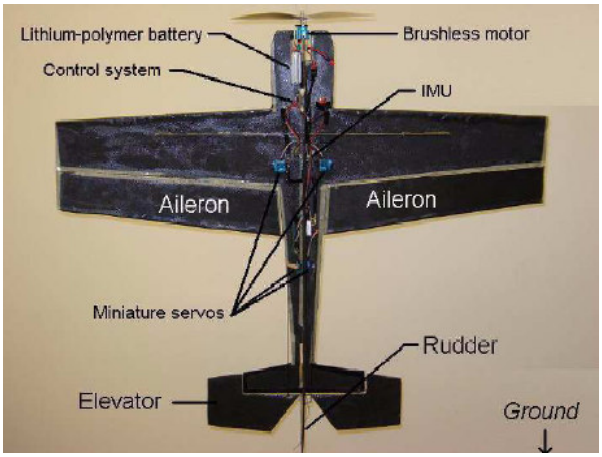

Figure 10: Drexel hovering fixed wing MAV [20]

The Maryland Active Structure Hovering MAV (see figure 11) [21] is a contra rotating coaxial design that uses shape memory alloys to deform the structure and provide translation. The design focus for this platform was to prove the technology, thus there has been minimal comment on actual flight performance.

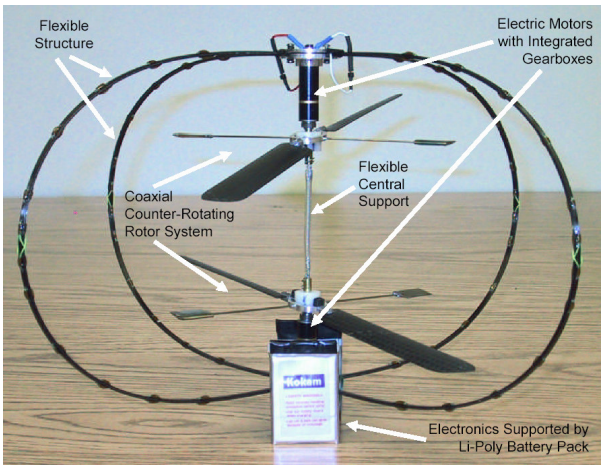

Figure 11: Active structure hovering MAV [21]

2.3 Platform Controllability Research:

Controllability is very important as it defines how manoeuvrable the platform will be. Here we will briefly discuss some of the possible options for controllability.

The first possibility is shape memory alloys (SMAs). They are limited by their bandwidth response and will only work at low frequencies typically 1Hz, thus making them unsuitable for blade deformation [22]. However, SMAs could be used for deforming the actual structure of platform, thus changing the angle of the rotors direction (see figure 12) [21]. However this would also require higher frequencies to be useful for

dynamic control. Operation requires heating of wire to trigger the SMA. To obtain the required heat a considerable amount of energy is dissipated and the effective change in length is only 3% of the total length.

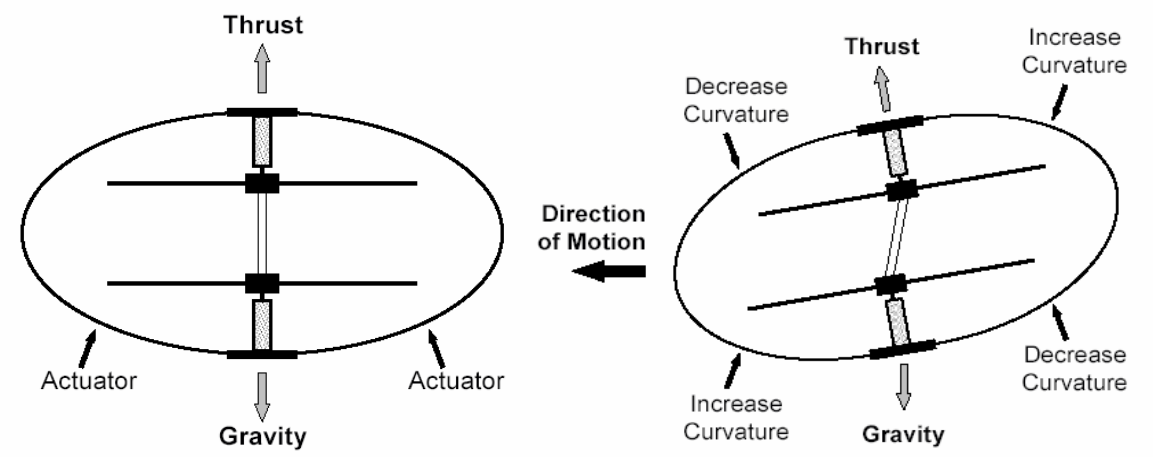

Figure 12: SMA structure deformation [21]

The second possibility is piezoelectric deformation, which has higher energy efficiency than the SMA, however, they can only provide small aerodynamic displacements [23] and they require high voltages for actuation. The technology behind the piezoelectric blade deformation is in its early stages and would require extensive research to get a usable design.

The third possibility is to use centre of gravity shifting to control the platform (see figure 13). However this method can introduce a pendulum effect and doesn't provide a very responsive control due to the dampening effect of the hinged mass [24].

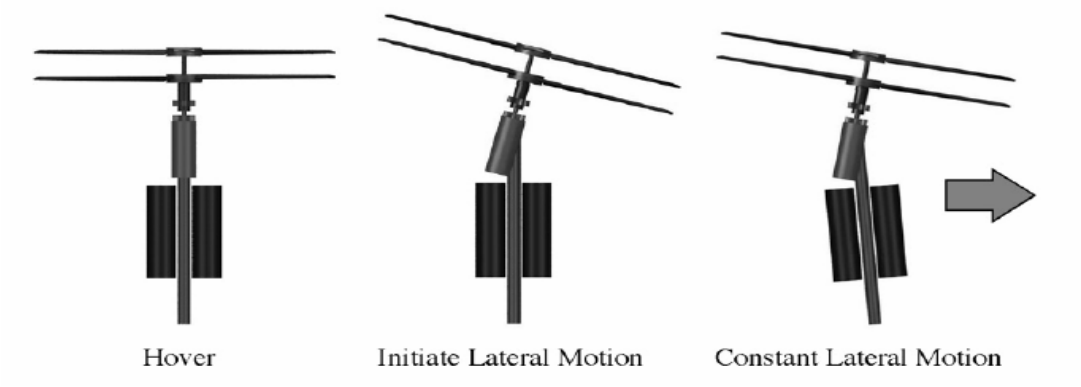

Figure 13: C.G shifting [24]

The fourth possibility is to place control vanes below the rotors to control the direction of the airflow (see figure 14) [17]. This system has a much higher actuation bandwidth (50Hz) than the previous which is determined by the response time of the servos, however, they can be difficult to mount depending on the platforms structure.

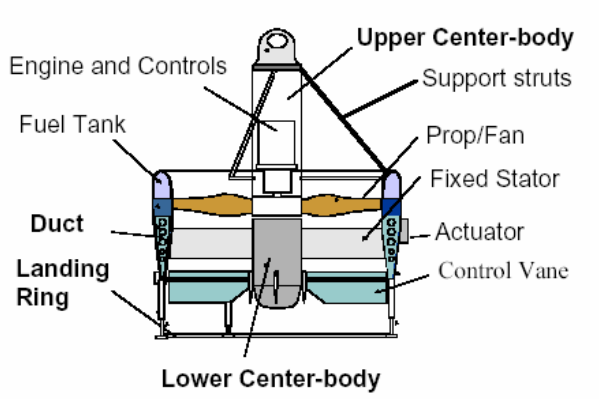

Figure 14: Control vanes [17]

The fifth possibility is to implement horizontal thrusters to tilt the platform towards the required direction of motion (see figure 15). However this method can also introduce a pendulum effect. It also does not provide a responsive control due to the large amount of thrust required to take the main rotors to a point of responsive behaviour [25].

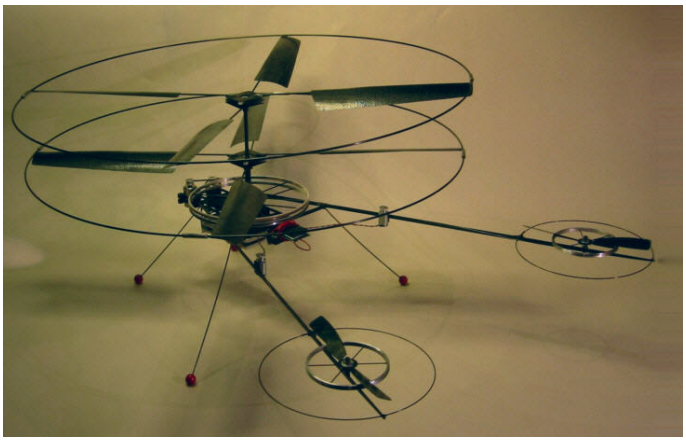

Figure 15: Contra-rotating coaxial helicopter with horizontal thrusters [25]

The sixth possibility is to utilise one of the most commonly used systems in both conventional and non-conventional designs, cyclic blade control (see figure 16). This method eliminates the need to fight against the main rotor. It has proven to be a very efficient way of manipulating the lift of the rotor and provide a very responsive control [26].

Figure 16: Cyclic blade control [27]

Based on this study the two most effective mechanical control methods studied are; control vanes and cyclic blade control, they both produce a responsive behaviour and are fairly efficient in design.

2.4 Advantages of Contra Rotating Coaxial Rotors:

These designs utilize all their power to drive two contra-rotating coaxial rotors. Yaw control is achieved by differential thrust between the two rotors. Thus no power is wasted in the horizontal plane on a tail stabilizer. Due to the second rotor they also have an increased lifting capacity. However, the lift is not quite doubled, when comparing the coaxial design with two separate rotors, for the same thrust the coaxial design requires approximately 41% more power [28].

On a conventional helicopter there is a condition called asymmetrical airflow in forward flight (see figure 17). If the rotor is spinning clockwise and the helicopter moves forward from a point of hover, it will have a rolling tendency towards the retreating blade. This is because the advancing blade has a higher airflow than that of the retreating blade [14].

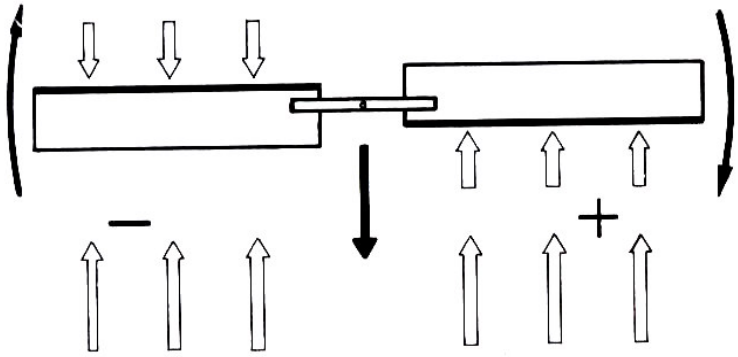

Figure 17: Asymmetrical Airflow [14]

In a contra-rotating coaxial configuration this effect is equal and opposite on each side and therefore the forces cancel out. This improves the stability of the platform.
The coaxial configuration can be contained in a much smaller more efficient and robust package than other more conventional configurations.

2.5 Preliminary Platform Testing:

The initial design stage aimed to discover the current capabilities of MAV platform technology in an attempt to unveil the best options in developing an appropriate and efficient final system. Here we will take a look at both fixed wing and hovering platforms to get an overall view on possible performance from the latest brushless motors, lithium polymer batteries and strong light weight materials;

2.5.1 The AstroFlyer:

The AstroFlyer is a fixed wing design based around a traditional biplane configuration (see figure 18). It was fabricated from depron foam with carbon fibre reinforcing. It possesses extraordinary manoeuvrability for a fixed wing, with a large wing surface area giving it increased lifting capacity and longer flight times. (***See videos; "AstroFlyer-Vid1", "Astroflyer-Vid2"***)

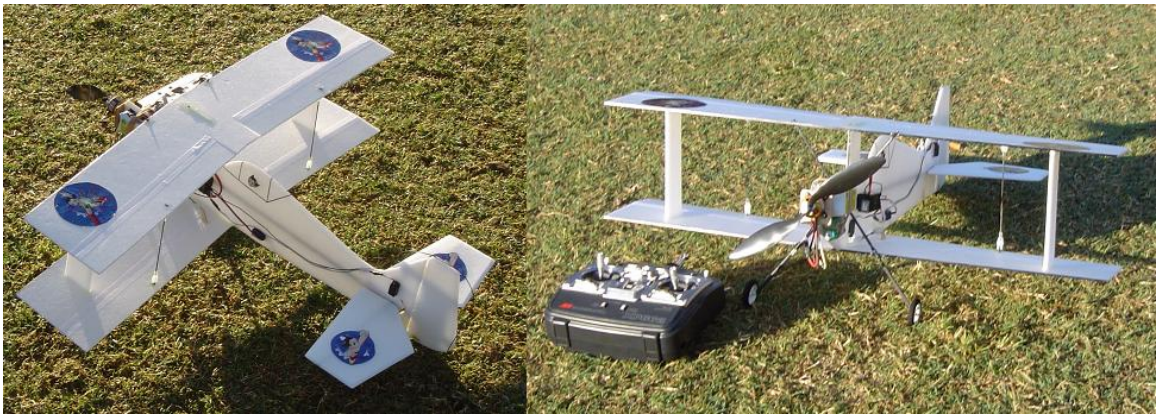

Figure 18: AstroFlyer Biplane

The AstroFlyer proved that it is possible to fly vertically and hover with a fixed wing configuration with relatively good control. However vertical flight reduces the flight time from 20min down to 3min. An expensive high precision IMU would be required to keep the aircraft flying vertically and would have problems with drifting.

2.5.2 The AstroWing:

The AstroWing is a fixed wing design based around the flying wing configuration (see figure 19). It was fabricated from depron foam with carbon fibre reinforcing. For a flying wing it possesses extraordinary stability and low speed flight characteristics. This was achieved by using a small un-aggressively pitched propeller, and by moving the C.G forward to allow for a constant elevator trim and increased angle of attack. The 'D' shape of the wing and aerofoil cross section improved slow flight and stable control.

Figure 19: AstroWing

The AstroWing was intended for vertical take-off and landing experimentation, however, it was unable to fly vertically due to the lack of aileron control to counter act the torque effect. It did however prove that it was possible to fly at a very slow speed with high

stability. It also provided a good platform for a wireless video camera. (***See videos; "AstroWing1", "AstroWing2", "AstroWing-CamForward", "AstroWing-CamBackward"***)

2.5.3 The Lampshade:

The Lampshade is a hovering platform design based around the rotating body, gyroscopically stabilized configuration (see figure 20). It was fabricated from depron foam with carbon fibre reinforcing. The platform proved it is difficult to fabricate a perfectly circular shape with perfect symmetry. Control was limited; only altitude could be controlled.

Figure 20: The Lampshade

The Lampshade proved that it was possible to gain stability directly from gyroscopic forces much like a spinning top. However a rotating body is very difficult to control in the x and y planes. (***See "Lampshade" video***)

2.5.4 The Flying Motor:

The Flying Motor is another hovering platform design, based around the rotating body gyroscopically stabilized configuration (see figure 21). It was fabricated purely from thin plywood. Control was limited; only altitude could be controlled.

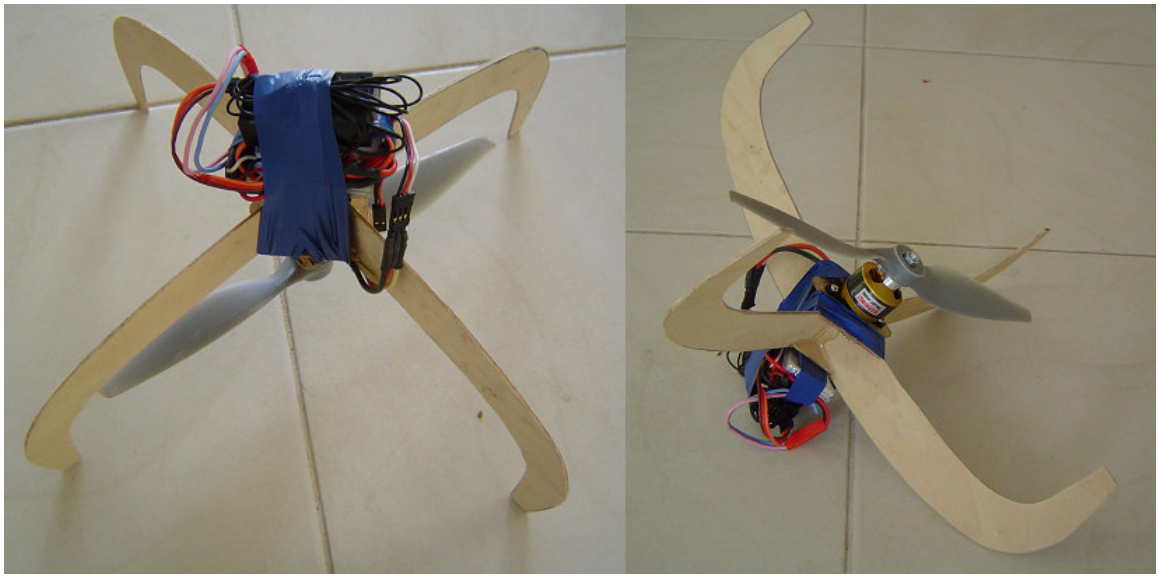

Figure 21: Flying Motor

The Flying Motor was designed to find the minimum physical requirement and simplest design for stable hovering capabilities. It possessed good efficiency, stability and a high power to weight ratio. However, due to the continuous rotation, controlling the direction of flight would require a complex cyclic paddle and it would be extremely difficult to fit useful external sensors. (***See "Flying Motor" video***)

2.6 Selected Platform Design:

After comparing all the platforms outlined above a comparison (Table 1.) was done to determine the best choice for our base platform. We can see that there is one platform that shows good results in every category including size, weight, controllability, manoeuvrability, efficiency and endurance. The commercial product of choice would be the Twister Bell-47, which possesses a good balance between stability and controllability. By choosing a somewhat neutrally inherently stable design, the complexity of the critical sensors and required processing power of the stability control system is greatly reduced.

Table 1: Platform Comparison

Name:	Image:	Operation:	Weight:	Size:	Hover Controlability:	Maneuverability:	Efficiency:	Endurance:	Payload:
Blade Runner		Indoor	~50g	~300mm	Easy	Bad	High	~5min	~5g
X-UFO		Indoor/Outdoor	~300g	~600mm	Complex	Excellent	Medium	~15min	~150g
Twister Bell-47		Indoor	~200g	~360mm	Medium	Good	High	~15min	~50g
Coander Effect		Indoor/Outdoor	~500g	~600mm	Hard	Good	Low	~10min	~50g
iStar		Outdoor/gas	~1.8kg	~230mm	Hard	Good	High	~1hr	~500g
MD4-200	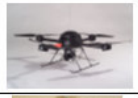	Outdoor	~800g	~900mm	Complex	Excellent	High	~20min	~300g
Drexel HFW		Indoor/Outdoor	~600g	~800mm	Complex	Good	Low	~5min	~100g
ASH Coaxial		Indoor	~200g	~500mm	Hard	Bad	Medium	~5min	~30g
AstroFlyer		Outdoor	~200g	~600mm	Complex	Good	Low	~10min	~100g
AstroWing		Outdoor	~100g	~400mm	NA	NA	NA	NA	NA
Lampshade		Indoor	~200g	~450mm	Easy	Bad	Medium	~5min	~50g
Flying Motor	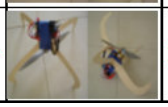	Indoor/Outdoor	~50g	~250mm	Easy	Bad	High	~10min	~100g

Chapter 3

3.0 Sensor Research:

The sensors are a very important part of any autonomous system and determine the degree at which the system interacts with the real-world and interprets its environment. Here two critical platform sensors will be discussed; the stability sensors and the altitude sensors.

The stability sensors are responsible for measuring the dynamic instabilities of the MAV and providing feedback to the stability controllers. The stability sensing and control system has to deal with the ever changing environment including platform instabilities and outside disturbances, thus it is required that these sensors are accurate.

The altitude sensing system is another integral part and is as equally important as the stability sensing system. This sensor is required to provide a hovering reference for the platforms vertical height.

3.1 Stability Sensors:

The ideal stability system would be able to keep the platform stabilised even when aggressive control commands are given by the pilot, so that as soon as the controls are released the platform would settle into a stable hover. This would allow the controls to be handed to an inexperienced pilot with minimal instruction. A mechanically stable

platform would provide a large degree of inherent stability, however, accurate sensors will still be required for robustness and autonomy. On an unstable platform accurate stability sensors are imperative.

There are several different types of sensors that can be used for inertial measurements including gyroscopes, accelerometers and magnetometers. Three gyroscopes are usually used to measure rotation about the x, y and z axis. By integrating the angular rate it is possible to compute the angle. Three accelerometers are usually used to measure acceleration in the x, y and z axis, this data can be used to determine velocity, distance and an attitude. Three magnetometers are usually used to give a reference measure to the estimated attitude of the platform. These sensors are available from a large range of suppliers in many different grades and packages.

In order to use all this information effectively some form of data fusion is required. A common method of data fusion is Kalman filtering [29]. Kalman filtering provides an estimate of the dynamic attitude by allocating weights to the different types of sensors depending on their qualitative ranges and bandwidth. Kalman filters are able to predict future estimations based on the current and past measurements. There are other simpler methods of data fusion, such as complementary filtering [30], that require less computation. Complimentary filtering uses high-pass and low-pass filtering to combine information from two sensors with different qualitative frequency regions. The performance of the complementary filter is not as good as the Kalman filter, however,

depending on the dynamic instabilities of the platform and control methodologies used they can be more than adequate.

The recent advancements in MEMS technology have enabled the development of extremely small, light weight inertial measurements units (IMU). There are many IMU devices available. The current world's smallest processor based inertial measurement unit is claimed to be made by Memsense [31]. The Nano IMU measuring 46mm x 23mm x 12.7mm provides digital temperature compensated outputs of triaxial angular rate, acceleration, and magnetic field data, for a full six degree of freedom system (see figure 22). Ranges of these sensors are between ±150 → ±1200 °/s for angular rate, ±2 → ±5g for acceleration and ±1.9 gauss for the magnetometer. There are two connectivity options; I²C and RS422. RS422 provides a robust differential link between the device and the flight computer that increases the immunity against noise. The sensor also comes in an analogue surface mount version (18mm x 18mm x 11mm) with no compensation or data formatting (MAG³) (see figure 22). However, they are extremely expensive and still require post processing to compute the attitude estimation. There are larger units that provide an attitude estimation output but they are too big for this project.

Figure 22: Left - nIMU, Right - MAG³ [31]

3.2 Altitude Sensors:

Two options for an altitude reference are; distance and a pressure sensors. The two main types of distance sensors are ultrasonic and infrared. Ultrasonic sensors are active sensors that provide an accurate distance to a reflective target by measuring the time of flight. Infrared sensors also provide an accurate distance to a reflective target by using triangulation. Triangulation is used to give accurate readings that are immune to different lighting conditions. Both types of sensors could provide an accurate displacement altitude reference from either the floor or the ceiling by measuring the time of flight. Ultrasonic sensors tend to work over larger distances and are lighter than the Infrared sensors.

The precision pressure sensor could provide an estimated altitude reference based on the ambient pressure where, the standard atmospheric pressure altitude equations are used to calculate pressure altitude. An improved version of this is to use the differential pressure to calculate an accurate altitude, where a second sensor is placed on the ground and the difference in pressure is converted to a relative altitude. This method is more accurate as the ambient fluctuations are present on both sensors. It does however require the ground sensor data to be transmitted up to the platform.

3.3 Selected Sensors:

On traditional UAV control systems a full IMU is used with a Global Positioning System (GPS). The IMU and GPS are integrated together with a Kalman filter to create an Inertial Navigation System (INS). This method works well as the position drift from the IMU is corrected by the GPS. Problems arise if the GPS signal is lost. Then the system on say a classical helicopter configuration would not be able to remain under full autonomy as the helicopter would not be getting accurate position corrections. This has been seen first hand at the International Aerial Robotics Competition (IARC) 2006 in Columbus Georgia USA, where the author attended and was a team member of Virginia Technology. With an indoor MAV control system this type of system cannot be used as the GPS signal is greatly attenuated and the affects of multi-path reflections are introduced when operating inside. There are some new GPS receivers that are designed for this type of situation however they are still relatively bulky (~100 mm x 60 mm) and expensive (~$6000 USD) for an MAV. Therefore alternate methods need to be introduced to work indoors.

This project adopts the idea of implementing a neutrally inherently stable platform so it will naturally and mechanically minimize the instabilities of the system without requiring precision attitude corrections. Tests were done initially to discover the minimum sensor requirements.

The sensors selected to be evaluated are:

- MEMS Gyros – Yaw, Roll and Pitch

- MEMS Accelerometers – X, Y, Z and Roll + Pitch Tilt Compensation
- Magnetometers and Electronic Compasses – Yaw
- Pressure Sensors – Pressure Altitude and Differential Altitude

A decision was made not to evaluate the Ultrasonic sensor for altitude. Some initial problems were foreseen that made it unsuitable for the applications required. The sensor provides an accurate distance between it and the object directly below it. The problem here is that if there was a large obstacle below, such as a table, then the platform would suddenly jump up in an attempt to keep the altitude distance correct. This is not ideal as it affects the outcome of the conducted experiment. With the pressure altitude sensor the platform would not be affected by such an object.

3.4 Sensors:

From the preliminary study the most appropriate sensors were chosen and linked to their specific control problem. The following sensors were mainly chosen for their availability, ease of use and low cost:

- MEMS Gyros – Yaw, Roll and Pitch (ADXRS300)
- MEMS Accelerometers – X, Y, Z and Roll + Pitch Tilt Compensation (MMA1260D, MMA2260D & MMA7260Q)
- Magnetometers/Electronic Compasses – Yaw (HMC1022)
- Pressure Sensors – Pressure Altitude and Differential Altitude (MPX4100A)

Due to the neutrally inherently stable platform design and its natural dampening of the pitch and roll rotational axis, a decision was made not to incorporate the gyros. This also beneficial to the reduction in cost and complexity of the system and promotes the minimalist approach. However, for yaw stability a gyro would still be useful.

These sensors were developed and tested independently before integrating them into 'The MicroBrain'.

3.4.1 MEMS 3D Accelerometer:

A 3D Accelerometer sensor board was fabricated to test the performance of the accelerometers ability to measure the attitude of the platform (see figure 23). Each single axis sensor has a built in second order Bessel switched capacitor filter [32]. The sensor can measure accelerations up to ±1.5G and has a sensitivity of 1200mV/G, with a 0G output of 2.5V.

The output of the sensor is fed into a first order filter to get rid of the high frequency noise generated by the internal switched capacitor filter. The signal is then read by the 16-bit ADC at any desired rate up to 100 KHz from the SPI interface. With the sensor range in mind (Δ3.6V) this gives an acquired resolution of: (3.6V / (5V / 65536)) / 3G → 15728.64 decimal points / G 'or' → **63.57828776 µG**. Equating to: **623.07 µms^{-2}**.

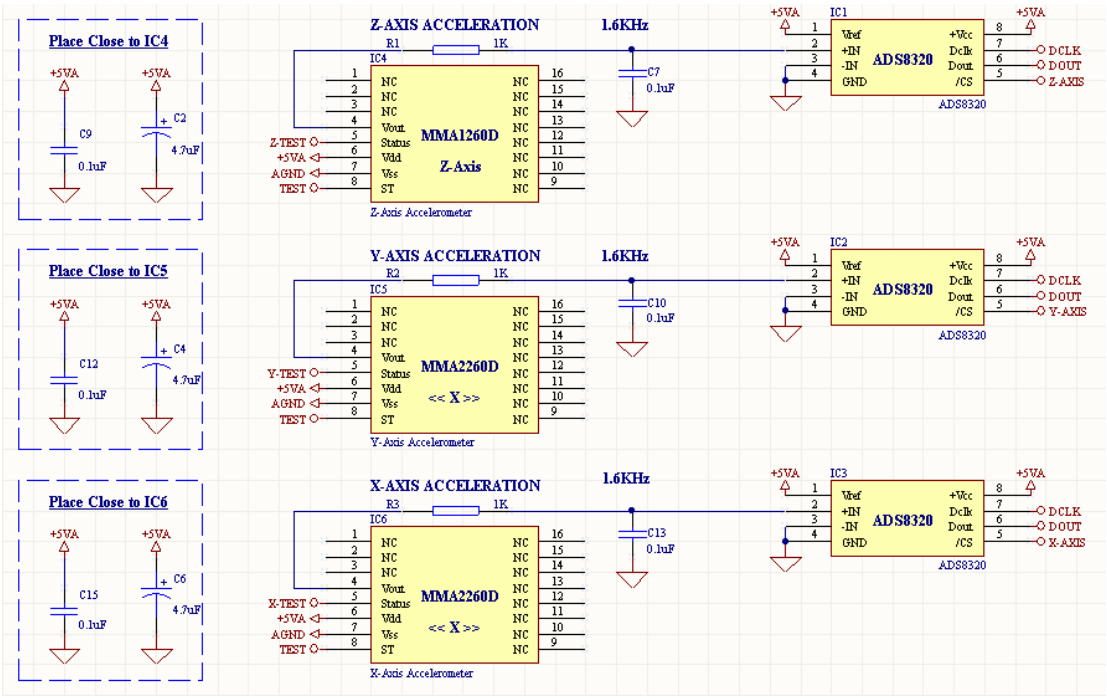

Figure 23: MEMS 3D Accelerometer Schematic

These ‘large’ sensors were supplied as free samples from ‘Freescale semiconductor’. The PCB was designed for the smallest and most compact size using this sensor package (see figures 24 & 25). One limitation to this was the accelerometers had to be aligned precisely in the x, y and z directions. The z-axis normally would require a PCB mounted vertically. Two accelerometer packages were chosen one with a horizontally placed sensor and the other with a vertically placed sensor to eliminate the need for a vertical PCB thus simplifying mounting.

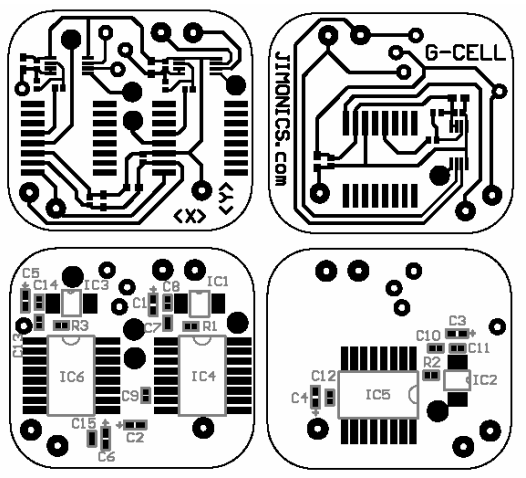

Figure 24: MEMs 3D Accelerometer PCB Layout (Not Actual Size)

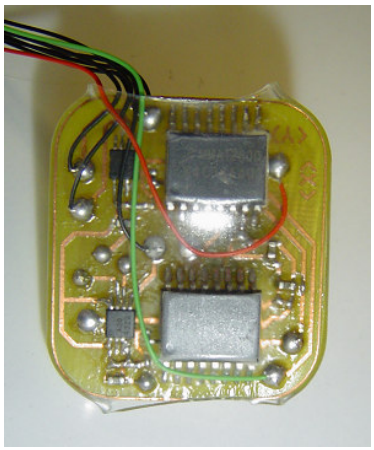

Figure 25: MEMS 3D Accelerometer Finished (20 mm x 25 mm)

3.4.2 2-Axis Magnetometer:

A 2-Axis Magnetometer sensor board was fabricated to test the performance of the magnetometer's ability to measure heading information (see figures 26 & 27). The schematic shows the 2-axis sensor, strap MOSFET, pre-amplifier and ADC. The two outputs of the sensor are fed into a pre-amplifier which also incorporates a low pass filter.

The signal is amplified by a factor of 1000. The signal is then read by the 16-bit ADC at any desired rate up to 100 KHz from the SPI interface.

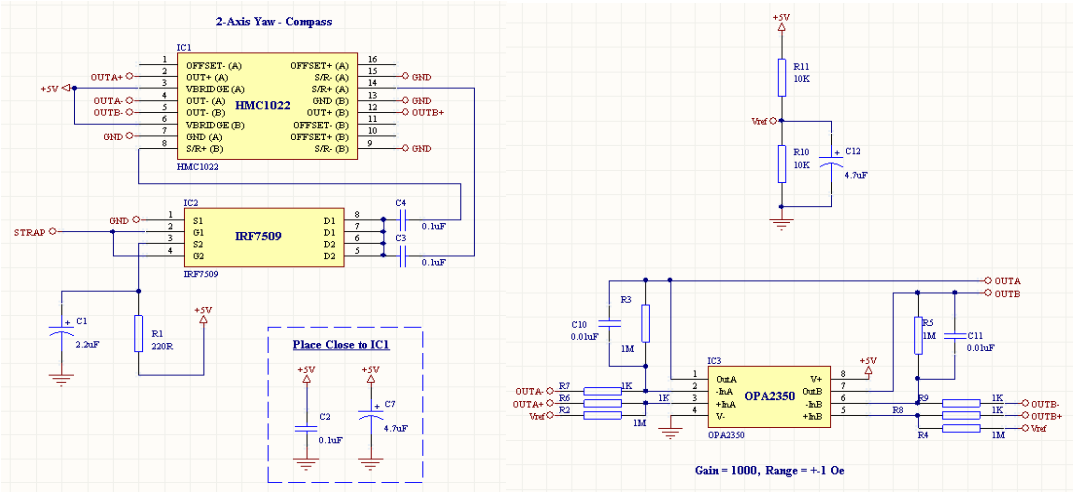

Figure 26: 2-Axis Magnetometer – Sensor & Op-amp Schematic

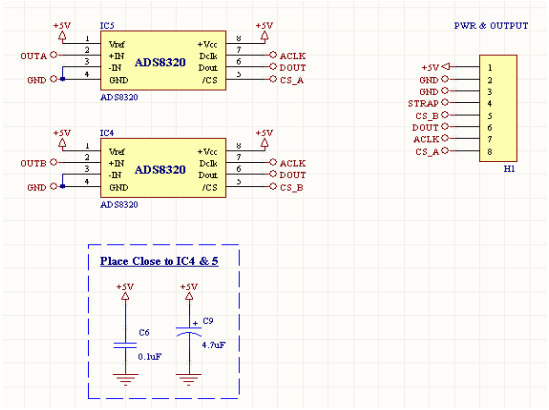

Figure 27: 2-Axis Magnetometer – ADC & Connector Schematic

The strap line is used to control the MOSFET transistor to energize the magnetic strap on each of the sensors (see figure 28). When a current is applied the magnetic domains are re-aligned within the actual sensor, thus re-sensitizing the sensor. This is necessary because when the sensor comes near any ferrous material the domains are scattered e.g. steel, iron, magnets, copper etc.

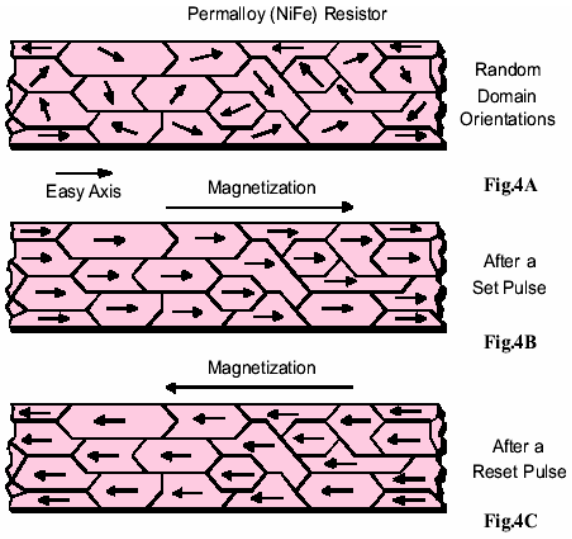

Figure 28: Domain Realignment - Re-sensitization [33]

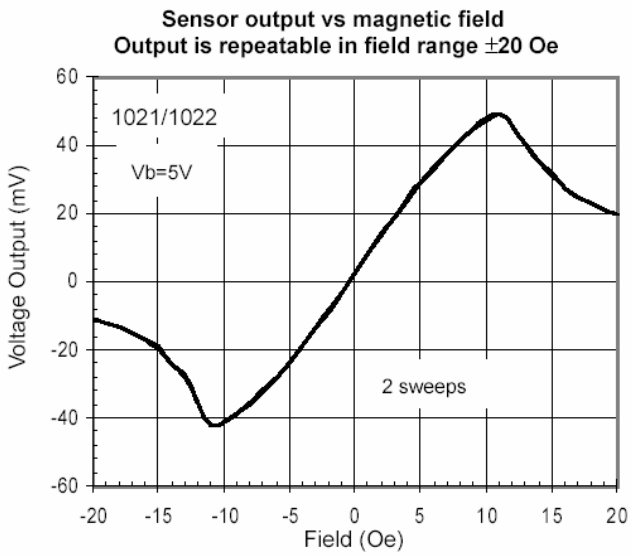

Figure 29: Sensor Voltage vs. Magnetic Field of the Earth [33]

From the data sheet, the sensors are specified to have a field range of ±6 gauss (The earth's magnetic field is roughly 0.5gauss) a sensitivity of 1 mV/V/gauss and a resolution of 85 μ gauss (see figure 29). This is the reason for amplifying by a factor of 1000. It is required to get a good range for the ADC which measures a voltage between 0V and +5V.

The Equation used to calculate the bearing from the two perpendicular sensors is as follows:

Equation 1: Bearing in Radians

$$Radians = atan2(X, Y)$$

Where, 'Radians' range from +Π to – Π. Then convert to degrees to give a compass bearing ranging from -180º to +180º:

Equation 2: Bearing in Degrees

$$Degrees = (Radians \times (\frac{180}{\Pi}))$$

The PCB was designed for the smallest and most compact package this is important as the placement of this sensor is critical (see figures 30 & 31). The board must be placed at least 200mm away from any ferrous material e.g. electric motors, gyroscopic bar weights and batteries. A small size and light weight is easier to mount this far from the centre of the structure as it would require less counter balancing and minimal support structure.

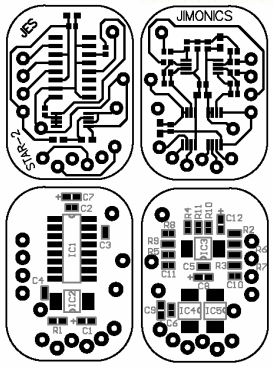

Figure 30: 2-Axis Magnetometer PCB Layout (Not Actual Size)

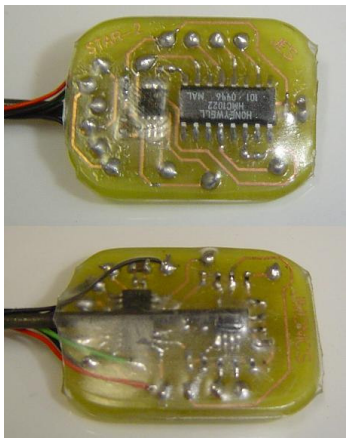

Figure 31: 2-Axis Magnetometer Finished (15 mm x 25 mm)

The finished sensor gave a very accurate reading of the bearing from 0º to 359º with an accuracy of approximately 2º and a resolution of approximately 0.1º.

3.4.3 Pressure Altitude:

An ambient pressure sensor board was fabricated to test the performance of the pressure altitude sensor and its ability to estimate altitude information. The board also provides both humidity and temperature readings for environmental corrections. The following schematic shows the car manifold pressure sensor, humidity sensor, temperature sensor, and ADC (see figures 32 & 33). The output of each sensor is fed into a first order low pass filter set to 100Hz. The ADC is supplied with a 2.5V reference voltage to set the range correctly. The signals are then read by the 24-bit ADC at any desired rate up to 20 KHz from the SPI interface.

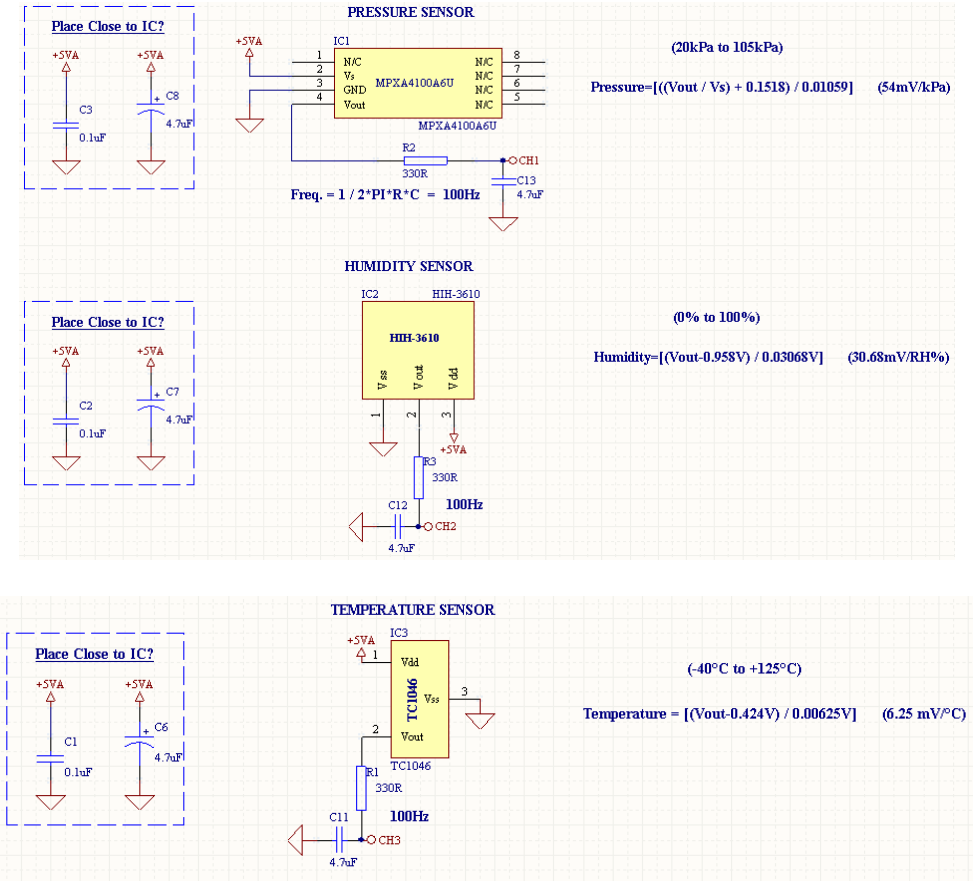

Figure 32: Pressure Altitude- Sensor & LPF Schematic

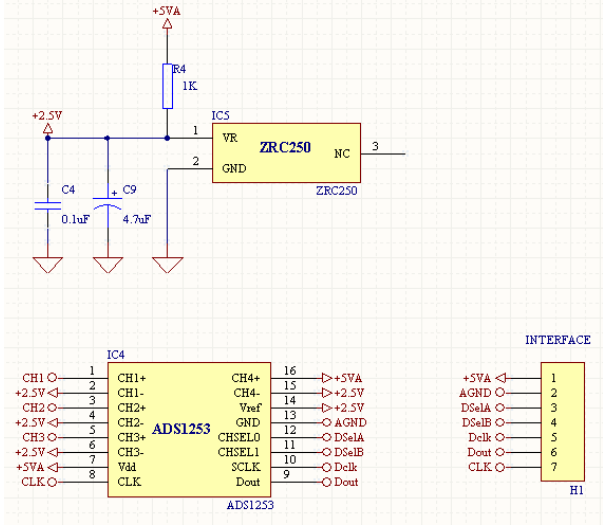

Figure 33: Pressure Altitude – ADC, Reference & Connector Schematic

Pressure Altitude Calculations:

The pressure sensor has a range between 20Kpa and 105Kpa which correlates to an altitude range between 11784m and -302 m respectively [34] (see figure 34). This is calculated using the standard atmospheric pressure altitude model based on air density (kg/m³), pressure (Pa) and temperature (K). When doing humidity and temperature corrections, the actual absolute humidity and temperature readings from the sensors are used. This gives a more accurate estimation of the altitude. The equations are derived from the ideal gas law equation [35]:

Equation 3: Standard Air Density

$$Air\ Density = \frac{Pressure}{(287 \times Temperature)}$$

Equation 4: Standard Temperature

$$Temperature = 288.16 - (0.0065 \times Altitude)$$

Equation 5: Standard Pressure

$$Pressure = 101325 \times \left(\frac{Temperature}{288.16}\right)^{\frac{9.80665}{287 \times 0.0065}}$$

Equation 6: Standard Humidity

$$Humidity = \frac{Pressure}{(461.5 \times temperature)}$$

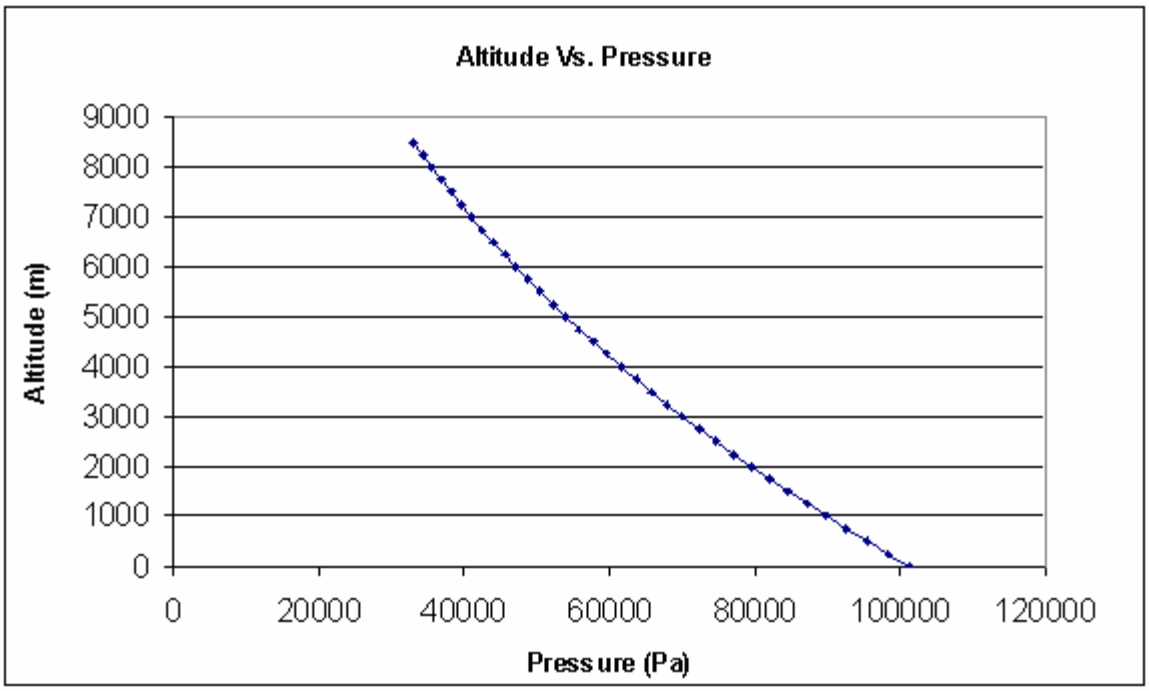

Figure 34: Altitude vs. Pressure - Standard Atmospheric Pressure Transfer Model.

The transfer functions of each sensor have been derived and are defined below:

Equation 7: Sensor Pressure

$$Pressure - [\frac{((\frac{Vout}{Vs}) + 0.1518)}{0.01059}](54\text{mV} / KPa)$$

Equation 8: Sensor Humidity

$$Humidity = [\frac{(Vout - 0.958\text{V})}{0.03068\text{V}}](30.68\text{mV} / RH)$$

Equation 9: Sensor Temperature

$$Temperature = [\frac{(Vout - 0.424\text{V})}{0.00625\text{V}}](6.25\text{mV} / ^{o}C)$$

On the top of the PCB the pressure sensor can be seen in the centre with the rectangular humidity sensor situated to the right (see figures 35 & 36). The temperature sensor, reference voltage and ADC can be seen beneath the board.

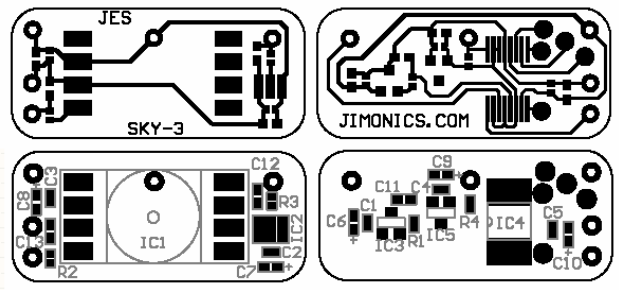

Figure 35: Pressure Altitude PCB Layout (Not Actual Size)

Figure 36: Pressure Altitude Finished (15mm x 35mm)

The finished sensor gave a very accurate reading of the altitude from -600 m to +11 km with an accuracy highly dependant on the weather and a resolution of approximately 50mm.

The above designs showed that it is possible to fabricate custom sensors with good performance and at low cost.

Chapter 4

4.0 Platform Stability:

The platform is neutrally inherently stable solely due to the actual mechanical design as discussed in detail in the initial study. However it still requires a stability control system to allow it to be fully autonomous and prevent the platform from flying off in a reactive direction.

The moments of rotation about the roll and pitch axes are somewhat dampened by the semi-articulated gyroscopic stabilisation system, thus reducing and, depending on the performance required, even eliminating the need for rate gyros on these axes (see figure 37). The attitude can still be calculated and represented with a co-ordinate system such as Euler Angles (see figure 38) using only acceleration measurements (inclination due to gravity), but you will have no high-frequency angular corrections from the gyros. It would be possible to increase the performance if a model of the dynamics, in particularly the rate dynamics, of the platform was estimated and used with these measured Euler Angles, however, it would be an extremely complex task to identify such parameters.

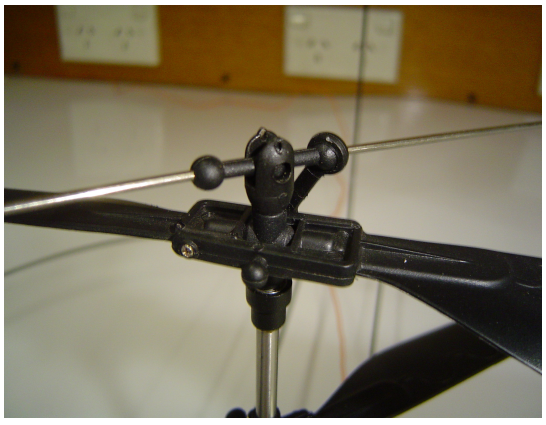

Figure 37: Top rotor stabilizer; showing 45° semi-articulated gyro activated arm

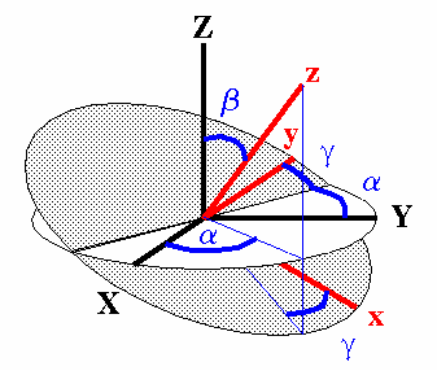

Figure 38: Euler Angles (α, β, γ) [36]

4.1 Stability Controller Selection:

Low level stability controllers together with a sensors and actuators are designed purely to stabilise the platform, without them the platform would be un-controllable. There are many different types of low level controllers. Here some of the most popular controllers used currently in both MAV and UAV systems will be discussed:

4.2 Proportional Integral Derivative Controller:

Proportional Integral Derivative (PID) [37] – This controller takes a measured value from a sensor and compares it with a set point. The difference between them is used to calculate the error. This error is proportionally multiplied by a gain factor kp. This provides the feedback required for the controller to respond to the immediate error. The integral term is a sum of the errors over time and is multiplied by the gain factor ki. This allows the controller to minimise the steady state error. The derivative term is the

difference between the current and the previous errors and is multiplied by the gain factor -kd. The PID controller can be tuned without a system model simply by changing these three gains (kp, ki & kd). The sum of each of these three terms is used to drive an output to correct the error (see figure 39). The PID controller can adjust its process, based on the history and rate of change of the error, giving an accurate and stable response. They do not require advanced mathematical processes and therefore have a reduced computational requirement. This type of controller is the most widely used in UAV and MAV applications.

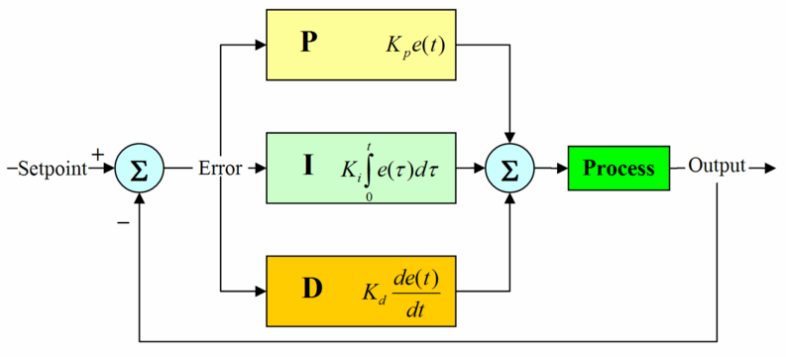

Figure 39: Basic PID Controller Block Diagram [37]

4.3 Linear Quadratic Regulator Controller:

Linear Quadratic Regulator (LQR) [38] – The LQR is based on the theory of optimal control, the goal being to operate a dynamic system at minimum cost. The system dynamics are described by a set of linear differential equations and the cost is described by a quadratic equation called the LQ problem with the weighting factors that are supplied. The "cost" of the system is judged by the sum of the difference of the error. The controller works to optimise this difference to a minimum. This type of controller is often not considered as it is a difficult process to find the correct weighting factors. It is a

computationally expensive process and requires an accurate model of the dynamic system under control. The LQR controller when optimized can provide excellent performance. This type of controller is mainly used for highly unstable platforms.

4.4 Neural Network Controller:

Neural Networks (NN) [39] – The NN has a parallel distributed processing structure that is loosely modelled after cortical structures of the brain. A number of interconnected processing elements called neurons work together to produce an output function. This output relies on the cooperation of the individual neurons to function correctly. A level of robustness comes from this parallel structure where the controller will still function even if some of the neurons are not working correctly. A network of agents is created that are collectively focussed on solving the control problem. They can be taught to deal with certain complex problems. A NN can be used with different learning algorithms to be trained to control a dynamic system without an accurate model of the system. The problem with this is that they can also learn 'bad habits' from the teacher and this process of learning can be difficult to setup on a flying platform.

4.5 Model Predictive Control Controller:

Model Predictive Control (MPC) [40] – The MPC is an advanced process controller that uses the empirical models of the dynamic system to compute the optimal control. The current measured inputs are used to calculate and predict the behaviour and future moves in the independent variables. The MPC then uses these to control the controller set points

and implement them into its process. The MPC is very computationally expensive. It requires iterative matrix algebraic calculations done at high speed and good precision.

4.6 Chosen Controller:

For a neutrally inherently stable platform, such as the Twister Bell-47, a standard PID controller would prove to be effective without diminishing performance. However for a platform like the X-UFO a more complex controller such as a NN or a LQR controller would be recommended, due to the high non-linear dynamic instabilities introduced by the design. Therefore the attitude and altitude control of the platform will be implemented with PID controllers. An evaluation will be made on their performance in *Chapter 8 - Operation Testing*.

Chapter 5

5.0 System Design:

Based on the information presented in the previous chapters a system design can now be created. The design would hold a balance between inherent stability and controllability for indoor use as an experimental test-bed. The development of some novel environmental sensors and state of the art inertial sensors could provide a stable base system for easy implementation of scientific experiments, with a real world demonstration of the performance.

5.1 Platform Design Solution:

The hovering platform design is based on the Twister Bell-47 toy helicopter. A Bell-47 was purchased and stripped down leaving only operational parts; rotor assembly, propulsion system, cyclic control assembly and actuation servos. This was necessary as the toy had many aesthetic parts that possessed no operational function. The original integrated receiver, gyro, mixer and speed controller were also removed. Doing this took off roughly 25% (50g) of its original weight which can be used as extra payload for the new hardware and external sensors. What was left became the centre piece of the design where a collision protection structure was attached as well as 'The MicroBrain' and magnetometer avionics equipment. This gave a goal payload of ~50g for the avionics and collision protection systems.

5.2 Propulsion System:

The propulsion system is described in two parts the: mechanical propulsion device and energy storage device:

5.2.1 Mechanical Propulsion Device:

The latest in mechanical propulsion devices are high efficiency brushless motors (see figure 40). Brushless motors, as the name suggests, have no brushes and therefore less friction and better electrical connectivity than the conventional brushed DC motor. It is common for brushless motors to achieve 70-85% efficiency. The Bell-47 already comes with two brushed motors.

It would be desirable to replace these with brushless motors however the mounting of the two is very different and would require heavy modification of the gearing system. Therefore a decision was made to simply use the motors provided.

Figure 40: Brushless Motor [41]

5.2.2 Energy Storage Device:

The latest most powerful commercially available battery technology is Lithium Polymer (LIPO) (see figure 41). They have a high energy density and are capable of supplying very large currents. Electric power is very reliable, efficient and clean. The platform has been fitted with a pack made from two LIPO cells in series (7.4V). The pack has more than twice the capacity of the original battery. Remotely piloted tests achieved a flight

time that was greater than 12mins fully loaded. Optimization for the balance between payload and flight time was done after the preliminary flight testing.

Figure 41: Single Cell Lithium Polymer [42]

The avionics were designed around the pack voltage so that the system only requires a single battery supply to run the entire system.

5.3 Collision Protection System:

A collision protection system is required to allow for small collisions that may occur during experimental testing indoors (see figure 42). The protection system needed to be able to absorb the shock during a collision without damaging the platform or preventing the platform from flying. A system was developed using thin carbon fibre rods arranged in a fashion so as to build a cylindrical structure around the centre piece. This structure also provides a good medium to mount 'The MicroBrain', magnetometer and external sensors. The structure had to be designed so it was light weight, yet strong, and a balance was met between structure rigidity and flexibility. Initially the two circles were made and then strengthened with perpendicular crosses. The two strengthened circles were then joined to form a cylinder using rods cut to appropriate lengths. The finished structure with centre piece can be seen below. (***See "Collision Test" video***)

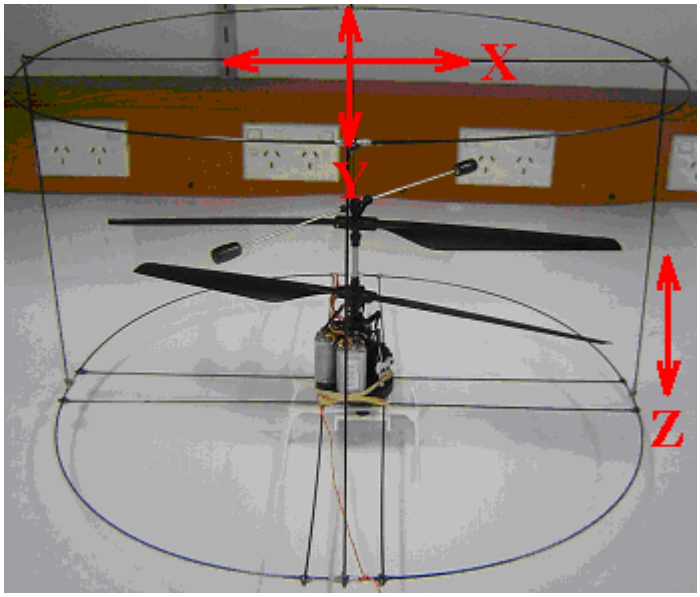

Figure 42: Collision Protection Framework

5.4 Platform Controllability:

The platform has four output devices that are simultaneously used to control the attitude and altitude of the hovering platform. These controls are grouped; motors and servos. The two motors drive the two rotors independently to transition vertically in the Z direction. The servos control the translation in the X and Y directions, aligned with the cage, with a dampened effect on the pitch and roll respectively (see figure 42).

5.4.1 Altitude Control:

Altitude is simply controlled by adjusting the collective thrust of both the rotor motors, where an increase in collective speed ascends the platform and a decrease in collective speed descends the platform.

5.4.2 Yaw Control:

Yaw is controlled by slightly adjusting the differential speeds between the two rotors. Increasing one rotor and decreasing the other rotor by the same amount will prevent altitude loss and also rotate the platform in a direction depending on the sum of the torques between the two rotors. This is in the opposing direction of the faster rotor.

5.4.3 X & Y Translation Control:

Translations in either the X or Y direction are achieved by simply adjusting the pitch and roll servos' actuation positions. The larger the deflection of the servo the faster the platform will translate. Note: The 45° + 45° precession affect as described in *Chapter 2*. The cyclic blade control is a method that has proven to be a very efficient way of manipulating the lift of the rotor, and provides a very responsive control.

The actuation controls are coupled to the bottom rotor by a mechanical device called a 'swash-plate'. The swash-plate alters the pitch of the blades cyclically to produce a net force 90° from the input (precession effect). The swash-plate has a bearing to allow for steady rotation between the controlled input and the blade control arm (see figure 43).

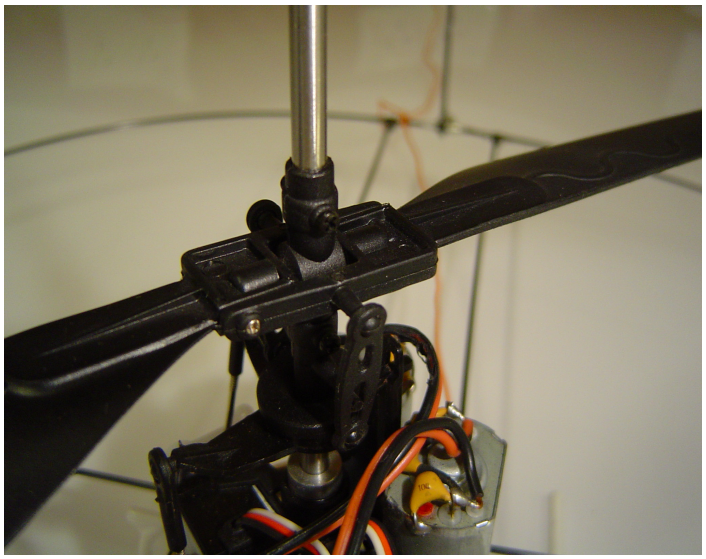

Figure 43: Bottom rotor; showing actuation arms, swash-plate & control arms

Chapter 6

6.0 Avionics Hardware Design:

The avionics hardware has some very exacting specifications which are critical in the pursuit of a seamless and complimentary platform and avionics design. The hardware has to be extremely light weight with a weight budget of ~40g. The flight computer must be less than 50mm x 50mm as a board any larger would cause airflow problems and difficult mounting on the MAV platform. In this section we will break down the avionics hardware and take a closer look at the main sections that form to create 'The MicroBrain' flight computer.

Note: All the lighter PCB's in the pictures were fabricated in a homemade double sided PCB lithography and etching lab specifically developed to have a minimum turn around for PCB designs (typically <1hr from schematic design to PCB realization).

6.1 Original R/C Electronics:

The original hardware on the toy platform incorporated a small PCB with an integrated; Radio Control (R/C) receiver, yaw gyro, two channel servo controllers, mixer and two channel speed controllers. Initially this board was going to be used as a base avionics package where the flight computer would tap into. By tapping in between the R/C receiver and the control section it is possible to trick the board into thinking it is talking to the R/C transmitter. This is done by decoding the PWM signals coming into the receiver from the transmitter and regenerating the PWM signals to feed into the control

section. This allows either; manual control by just regenerating the PWM signal coming in, or autonomous control by regenerating the desired PWM signals. An oscilloscope was used to trace the important parts of the circuit and work out the connectivity. A detailed picture showing connectivity can be seen below (see figure 44 & 45):

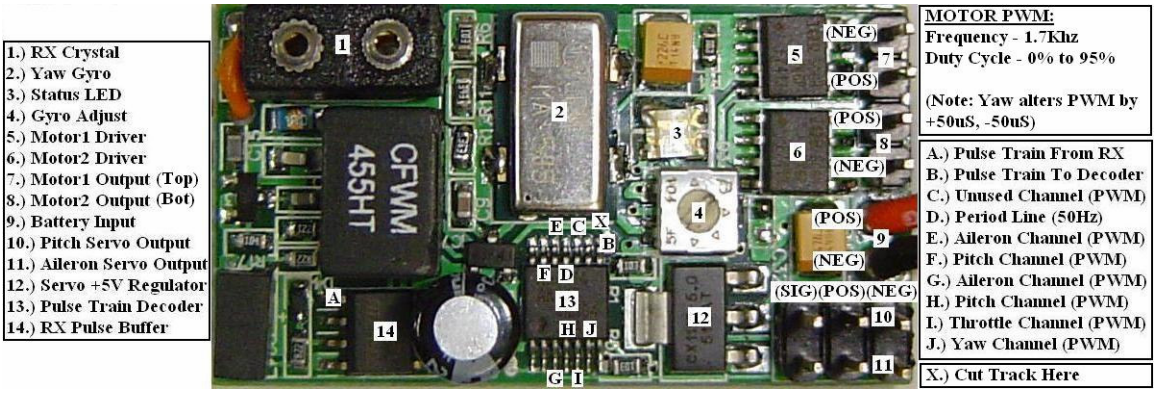

Figure 44: Topside of Original R/C Electronics

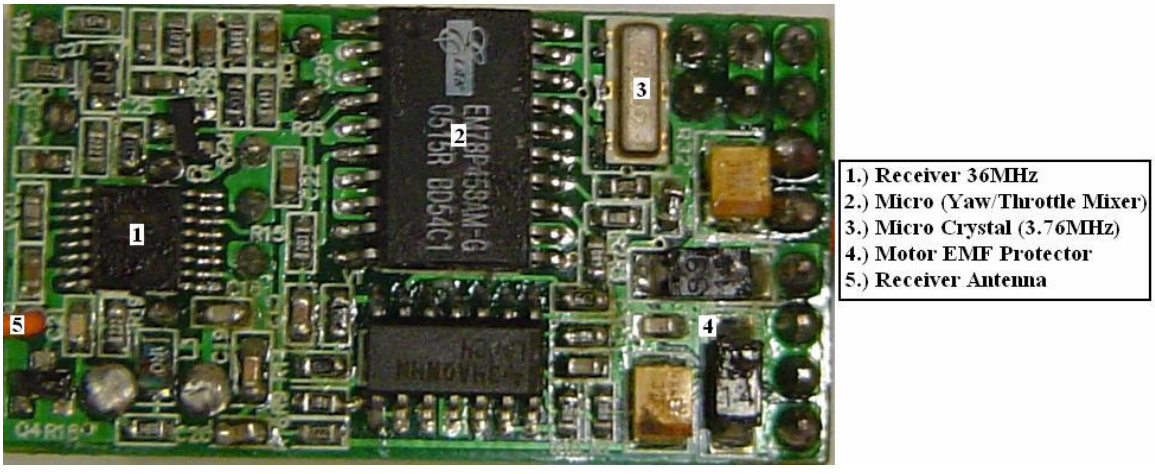

Figure 45: Bottom side of Original R/C Electronics

As you can imagine it would also be quite messy and unreliable, soldering wires from this board to connect to the flight computer. So it was later decided that a custom developed system was more desirable and allowed for easy debugging.

6.2 Data Acquisition:

The data acquisition system is an extremely important process that directly affects the performance of the entire system. Care must be taken when designing both the hardware and the software to achieve the desired; resolution, accuracy, anti-aliasing and speed. Most sensors, like the ones that were developed above, have analogue voltage outputs. In order for the processor to use this information it needs to be converted into the digital domain using an Analogue to Digital Converter (ADC).

Some guidelines for achieving good results are:

1. Use a High pass, Low pass or band pass filter, depending on the application, to reject all unwanted signals/noise (often the sensor data sheet will recommend an application circuit).

2. Use a high resolution ADC, depending on required results.

3. Use decoupling capacitors & good power regulation to reduce noise.

4. Use separate supplies for analogue and digital/noisy circuits.

5. Use a sampling frequency an order of magnitude (>2x) larger than the required system frequency, to eliminate aliasing.

6. Minimize the distance between the sensor and the ADC.

6.3 Central Processing Unit:

The processor will read the acquired data from the ADCs and convert that data into the desired format. This data is then fed into the controller and the output is used to control the actuator positions and speed of the electric motors. The processing speed in million instructions per second (MIPS) is directly related to the speed in which the system can run continuously, completing all the tasks mentioned above. As you can see the number of sensors, controllers and number of outputs, is the dividing factor of this processing resource. Therefore it is essential not to overload the processor by having a significant speed margin above the computational requirement to allow for any non cyclic tasks like manual control inputs from the remote control.

The refresh rate of the system needs to be an order of magnitude larger than the dynamic natural frequency of the platform's responsive behaviour. This natural frequency generally increases as the physical size of the platform reduces, due to the reduction of the platform inertia. If the natural frequency is an order of magnitude less than the refresh rate of the control system, then the responsive behaviour of the controller will be able to correct the attitude of the platform, thus aiding the platforms dynamic stability.

A study was done to find the most appropriate processor for stability control and communications including wireless, R/C and GUI interfaces. The computational requirements were increased due to the secondary requirement to read extra external sensors and process the guidance and navigational algorithms. This study became a choice between two of the leading microcontroller manufacturers; 'Microchip' and

'Atmel'. The current high end 8-bit microcontrollers were evaluated by developing a processing board and testing the performance based on; MIPS, Memory, Connectivity, physical footprint and C compiler. The two rival designs were:

6.3.1 Microchip – PIC18F252 [43]:

Specifications:

- **Processor**: PIC18F252 ($26)
- **Speed**: 10 MIPS
- **Memory**: 32 kb FLASH 1536 bytes RAM 256 bytes EEPROM
- **Connectivity**: 1x USART, 1x SPI or 1x I²C
- **Package**: SMD SOIC-28
- **Compiler**: PICC18 C Compiler –Microchip

Development Board:

This test board was developed with twin PIC18F252 processors onboard (see figure 46). Connectivity between the two processors was via the Serial Peripheral Interface (SPI). This left one USART port for connecting to the radio modem (*Seen beneath the top board*) and the other for external connectivity. This board has a built in 6 channel servo controller (*seen top right connector*) and 12x digital I/O connectivity for external sensors. (*Seen top & bottom connectors*)

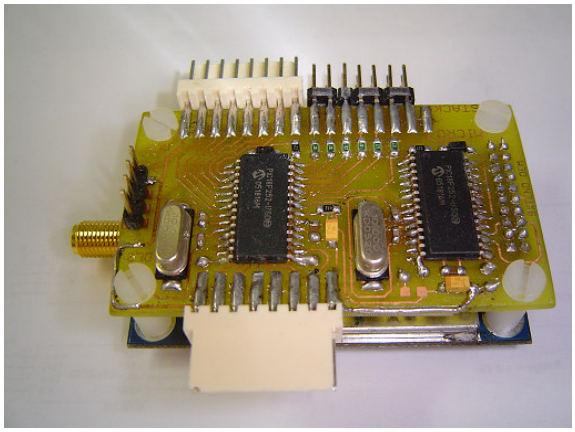

Figure 46: Microstack - 2x PIC 18F252

Pros:

- Built in servo controller
- 20MIPS Collective Processing Capability
- Designed to stack on top of the radio modem
- Onboard voltage management circuitry

Cons:

- Large due to SOIC-28 packages
- Bulky connectors
- Limited connectivity
- Tedious programming connectivity - interface clips on to individual pins
- Communication between processors
- Compiler inconsistent & not user friendly
- Comparatively expensive

6.3.2 Atmel – ATMEGA162 [44]:

Specifications:

- **Processor**: ATMEGA162 ($13)
- **Speed**: 16 MIPS (two cycle multiplier)
- **Memory**: 16 kb FLASH 1000 bytes RAM 512 bytes EEPROM
- **Connectivity**: 2x USART, 1x SPI, 1x JTAG
- **Package**: SMD TQFP-44
- **Compiler**: Code Vision C Compiler

Development Board:

This test board was developed with a single ATMEGA162 processor onboard however up to 32 modules can be stacked to create a powerful distributed processing system (see figure 47).

Connectivity between the processors is via a RS-485 bus (*USART port 1- Seen Figure 47, bottom black connector*). This left one remaining USART port for each board in the stack for external connectivity (*Seen left solder pads*). Each board has 16x digital I/O connectivity for external sensors (*Seen top & right solder pads*). The programming interface is via the small white SMD connector (*Seen left*).

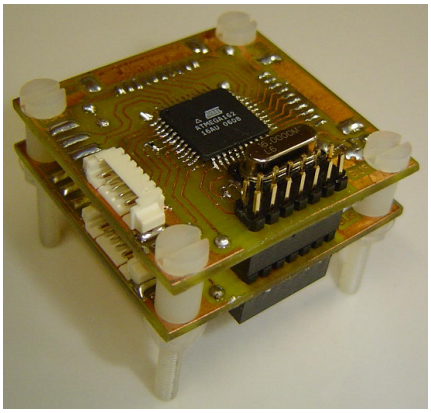

Figure 47: Microstack – 2x ATMEGA162

Pros:

- 2Mbps RS-485 BUS allows 32 boards to be connected together
- 16MIPS to 512MIPS Collective Processing Capability
- Two USART port per chip
- Onboard voltage management circuitry
- Easy programming connectivity
- Small and compact package
- Good, easy to use and reliable C compiler
- Two cycle multiplier
- Large EEPROM
- Comparatively inexpensive

Cons:

- Less FLASH and RAM

6.3.3 Chosen Processor:

The chosen processor was the 8-bit 'ATMEGA162' manufactured by 'Atmel. This processor was chosen as it has good connectivity, is 60% faster and has an easy to use, reliable compiler. The package size is smaller and easy to implement and the chip costs half as much as the competitor's.

6.4 Control Actuators:

The control of the servo actuators is achieved using Pulse Width Modulation (PWM) techniques. The standard servo incorporates a small electric motor which is geared up for increased torque. They have a variable resistor which is used as a feedback sensor for accurately positioning the output shaft. Servos are most commonly used in radio controlled equipment.

There are three leads connected to a servo. Two supply power to the servo +4.8V (+4.00V → +6.00V) and GND. The third is the PWM signal that tells the servo what position to hold. The signal pulse width ranges from 1mS → 2mS over a 20mS cycle (*50Hz*) (see figure 48).

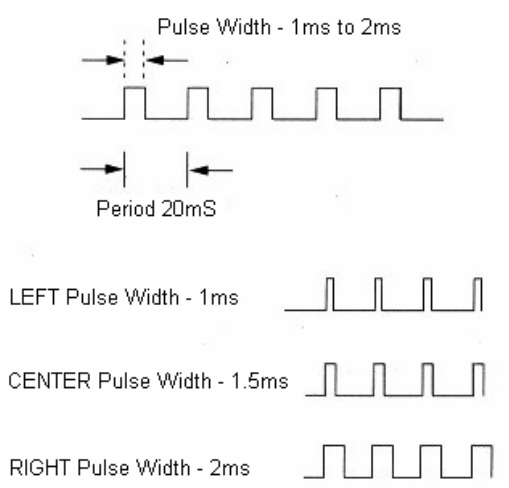

Figure 48: PWM Signal Timing Diagram

The task of accurately generating and monitoring these PWM signals can be computationally expensive. Therefore a servo controller module called the SCM-18 was developed to encode these PWM signals to minimize the computational requirement and take the complexity away from the flight computer (see figure 49 & 50). The SCM-18 is a complete servo controller that you can easily connect to the flight computer via a USART communications port. Its small size allows it to be used even on MAV projects. Its low power consumption and light weight increase its portability to battery powered systems. The SCM-18 has the capability of storing failsafe servo positions in its internal non-volatile memory, thus increasing the safety levels by preventing motor run away and drastic actuation positions in the case of a flight computer failure. The pulse width modulated output signals have 200nS precision. That gives your servo an amazing 5000 different position increments over the servos' range. Up to 248 servos' can be controlled from one serial port. The simple message protocol makes it very easy to manipulate the servos and motor speed controller. The SCM-18 was developed, and is now produced commercially by the Jimonics [45].

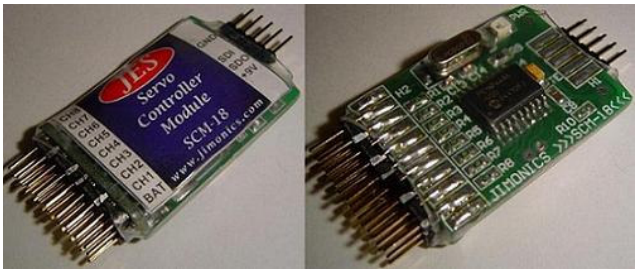

Figure 49: SCM-18

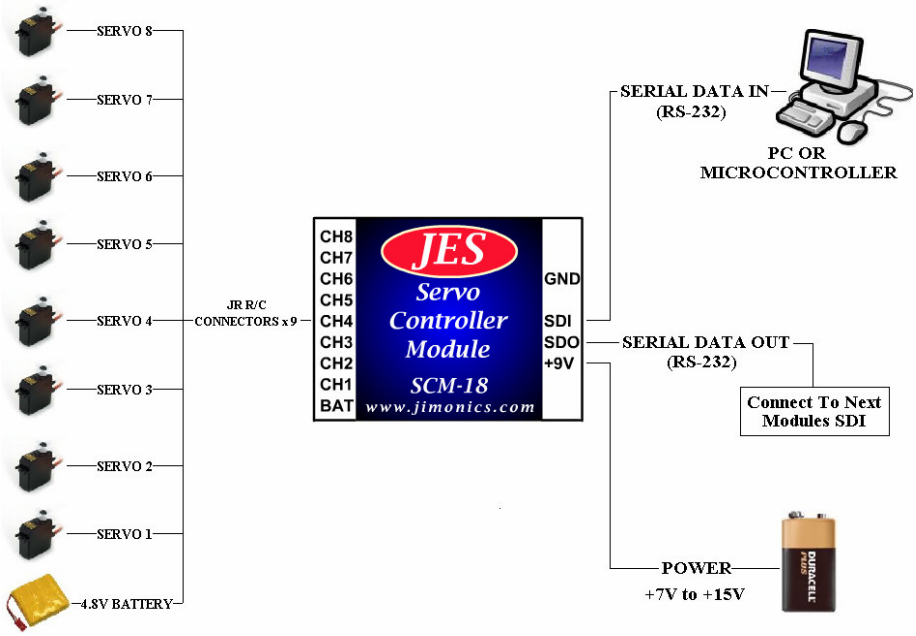

Figure 50: SCM-18 Functional Diagram

6.5 Propulsion System:

Control of the electric motors is also achieved using Pulse Width Modulation (PWM) techniques but there is a significant difference in the frequency and duty cycle. A motor speed controller is used to convert the PWM signals from the servo controller to the higher frequency (typically 2.5 KHz) PWM signals required to control the DC motor. Therefore two small 'Skyborne 14' motor speed controllers were purchased to allow the SCM-18 to control the propulsion system (see figure 51). This device also incorporates a Battery Eliminator Circuit (BEC) and a battery monitoring circuit, which are used to power the two servos, and prevent the battery discharge voltage to going below their respective minimum cell voltage. They measure 21mm x 11.5mm x 7.1mm weighing only 6.7g.

Figure 51: Skyborne 14 Motor Speed Controller [46]

6.6 Communications:

Several types of communications systems were evaluated including; 900 MHz 9-Xtend Radio Modem & 2.4 GHz Xbee Radio Modem by Maxstream and the 2.4 GHz Wiport by Lantronix. The evaluation of each is focused on; frequency, size, weight, datarate, power consumption, connectivity and cost. Range was not regarded as critically important due to the fact that the platform will be flying indoors.

6.6.1 9-Xtend [47] (see figure 52):

Specifications:

- **Frequency**: 900 MHz
- **Size**: 60.5mm x 36.5mm x 5.1mm
- **Weight**: 18g
- **Datarate**: 115 kbps
- **Power Consumption**: 3650mW
- **Connectivity**: USART (Networking Capability)
- **Cost**: $260ea (AUD)

Pros:

- Good skin depth due to lower frequency (Can penetrate walls better)
- Light weight

Cons:

- Large Size
- High power consumption
- Expensive

Figure 52: 9-Xtend Radio Modem

6.6.2 Xbee [48] (see figure 53):

Specifications:

- **Frequency**: 2.4 GHz
- **Size**: 32.94mm x 24.38mm x 3mm
- **Weight**: 4g
- **Datarate**: 115 kbps
- **Power Consumption**: 709.5mW
- **Connectivity**: USART (Networking Capability)
- **Cost**: $30ea (AUD)

Pros:

- Small size
- Extremely light weight
- Low power consumption
- Built in Advanced Networking Functionality
- Inexpensive

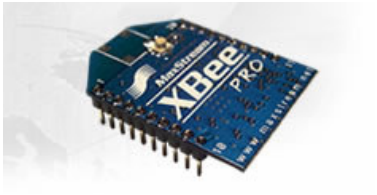

Figure 53: Xbee Pro Radio Modem

6.6.3 Wiport [49] (see figure 54):

Specifications:

- **Frequency**: 2.4 GHz
- **Size**: 33.9mm x 32.5mm x 10.5mm
- **Weight**: 29g
- **Datarate**: 921.6 kbps
- **Power Consumption**: 1300mW
- **Connectivity**: USART (WIFI Networking Capability)
- **Cost**: $160ea (AUD)

Pros:

- Small size
- High datarate
- Full WIFI stack with Advanced Networking and Security

Cons:

- Heavy
- High power consumption
- Expensive

Figure 54: Wiport WIFI Module

6.6.4 Chosen Communications System:

The chosen communication system was the 'Xbee-Pro' manufactured by 'Maxstream'. The Xbee was found to be the perfect solution as the package size and weight is extremely small. Its built-in advanced networking functionality makes it very easy to implement and secure. The cost of these modules is a fraction of the competitor's. It also has the best power consumption allowing the autonomous platform increased flight time.

6.7 The MicroBrain:

The MicroBrain is an integrated solution derived from research and developments presented in the preceding chapters. It has been optimized for size, weight and increased functionality. The specifications of the MicroBrain are as follows:

6.7.1 Specifications:

- Atmel 16MIPS Processor – IDE C-Code
- RC Pulse Train Decoder
- USART Connectivity
- SPI Port – 8 External 16-bit ADC Connectivity
- Xbee 2.4GHz Wireless Communication – With Networking
- Integrated 3D Accelerometers
- Integrated Pressure Altitude Sensor – Differential Altitude Capability
- Onboard Battery Monitor – LIPO 2 to 3 cells
- Size: 45mm x 35mm x 11mm

- Weight: ~11g
- Generic Design - Doubles as a Ground Station

  (The ground station was fitted with USB Connectivity)

The block diagram of the system below shows the processors allocation of physical resources and connectivity to sensors, actuator and motors (see figure 55):

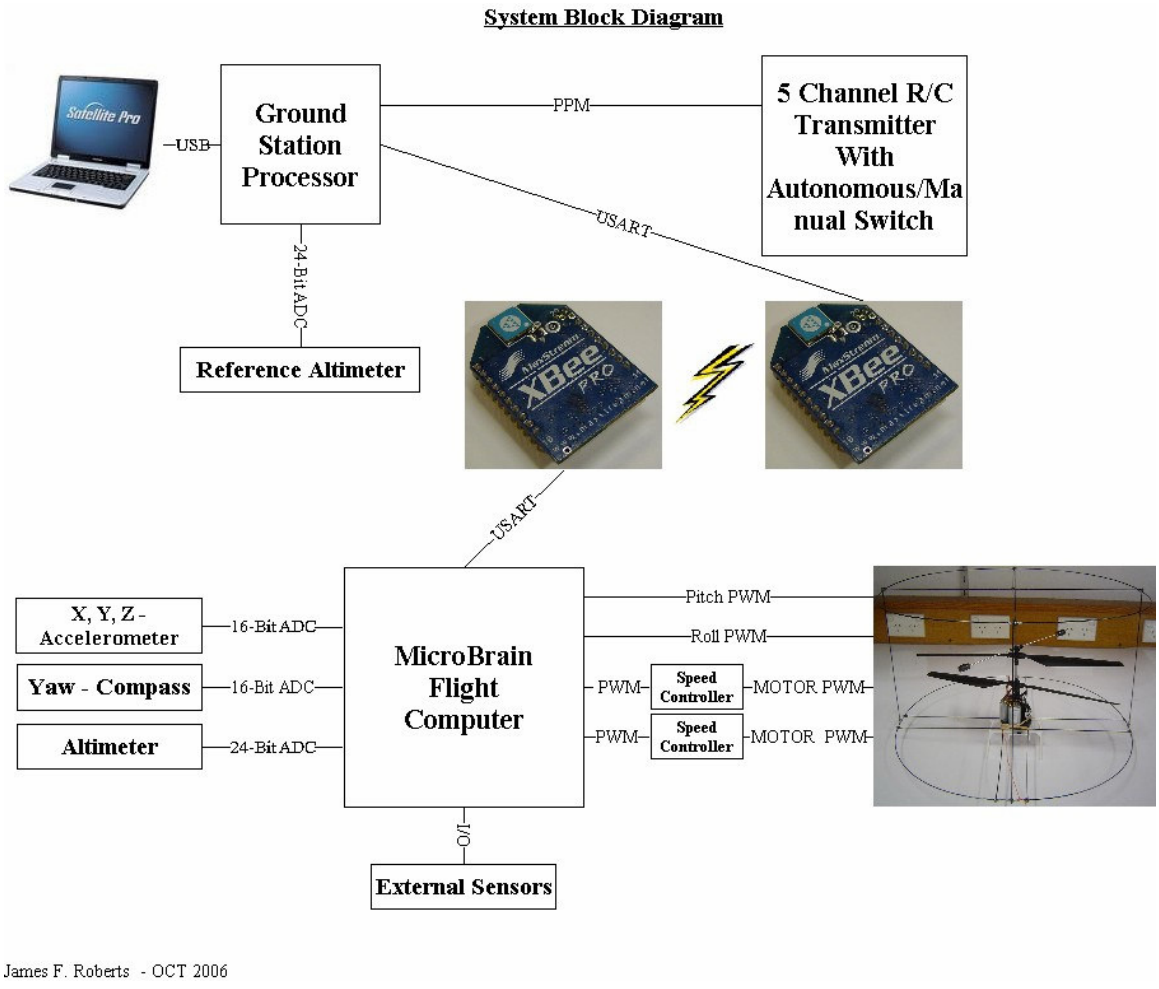

Figure 55: The MicroBrain System Block Diagram

6.7.2 Schematics:

The schematics of the MicroBrain show the support circuitry that surrounds the microcontroller. There are two voltage regulators; 3.3V and 5V (see figure 56). The digital and analogue circuitry is separated using a simple current limiting technique employing a strategically placed resistor. The 3.3V supply powers the 3-axis accelerometer, 16-bit ADC Reference, Analogue Multiplexer and Xbee Modem. The 5V supply powers the Microcontroller, Pressure Sensor, 24-bit ADC and the 16-bit ADC.

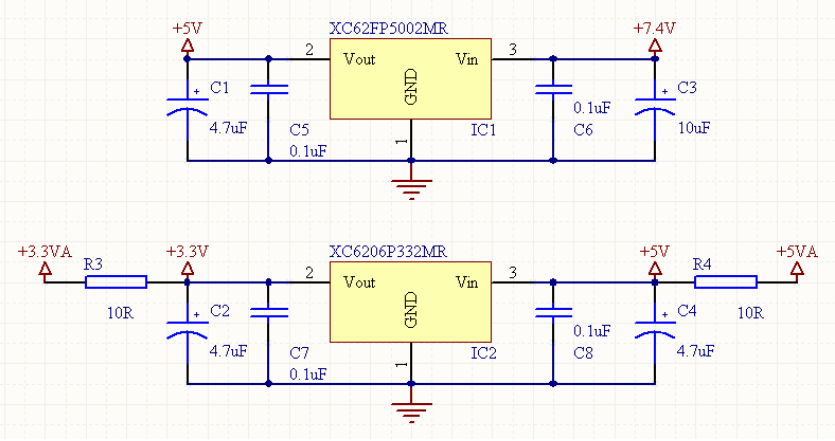

Figure 56: Power Supply

The accelerometer sensor has a built in switched capacitor filter which provides the required filtering for acquisition (see figure 57). However due to the nature of this type of filter a high frequency first order filter is required to eliminate the high frequency created from the switching. This sensor works in a similar manner to the accelerometer already evaluated but it's been packaged into a SMD QFN-16 chip that measures only 5.5mm x 5.5mm x 1.45mm. The sensor allows you to select a 'g' rating of; ±1.5g, ±2g, ±4g and ±6g. The sensor was set to the minimum 'g' rating for maximum sensitivity. A

simple voltage divider monitor was also incorporated to measure the battery health during flying (see figure 58). These four analogue signals are then fed into an analogue multiplexer so a single 16-bit ADC can read all outputs (see figure 59). The microcontroller communicated with the ADC via a custom SPI port.

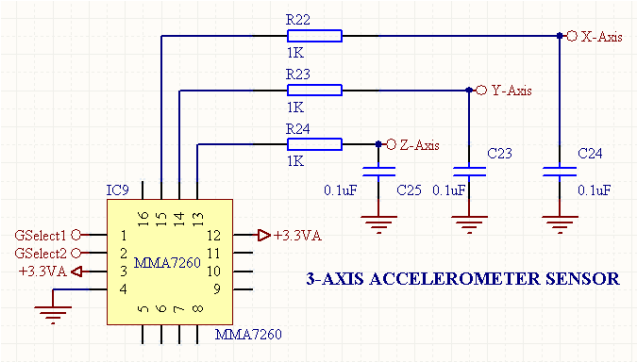

Figure 57: 3-axis Accelerometer

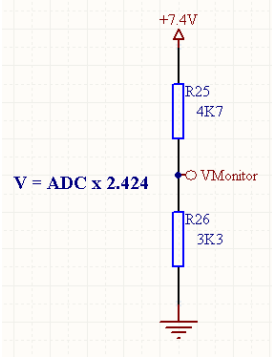

Figure 58: Battery Monitor

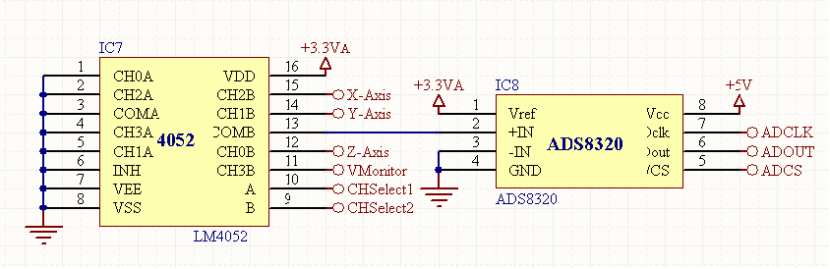

Figure 59: Analogue Multiplexer & 16-bit ADC

The pressure sensor has a first order low pass filter (LPF) set to 10Hz in order to minimize high frequency interference and prevent aliasing. This is then fed into an ultra high resolution 24-bit ADC to measure a theoretical altitude resolution of 7mm however this is limited by the sensors resolution (see figure 60). The microcontroller communicates with the ADC via a custom SPI port. To gain this kind of resolution the ADC employs a Sigma Delta Architecture which requires a high frequency clock to set the internal digital FIR filter. The -3dB cut-off of this filter was set to 100Hz which equates to a 38.4 KHz clock. The clock is supplied by a PWM generator onboard the microcontroller.

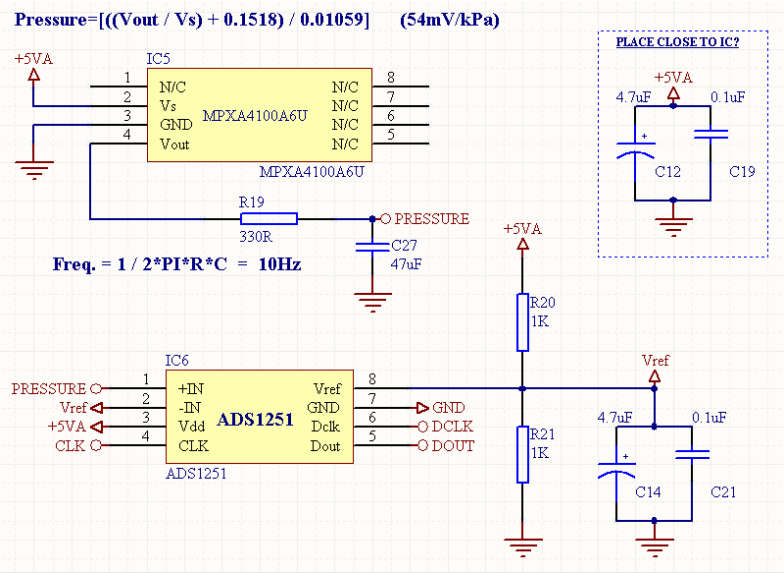

Figure 60: Pressure Sensor & 24-bit ADC

There is an external digital interface to connect with up to eight external 16-bit ADC or digital inputs (see figure 61). This is the interface for the external sensors including the

2-axis Magnetometer. The I/O ports are current limited to prevent accidental damage to the internal transistors.

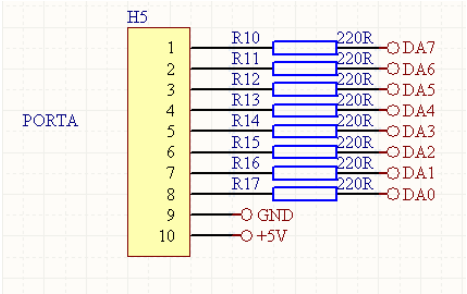

Figure 61: Digital I/O

There is connectivity for selecting between Autonomous and Manual modes if the radio control only has four channels (see figure 62).

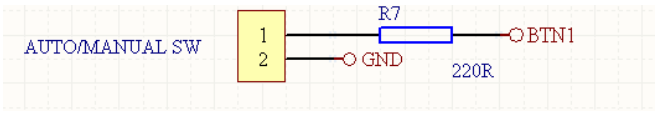

Figure 62: Alternate Autonomous Manual Switch

The MicroBrain was designed to be a generic board able to work as either the onboard flight computer or the ground station. Naturally the ground station was not fitted with the accelerometers or multiplexer. The ground station was however also fitted with USB connectivity to allow easy connectivity to a Laptop computer. The USB provided the power for the ground Station so no external power was required (see figure 63).

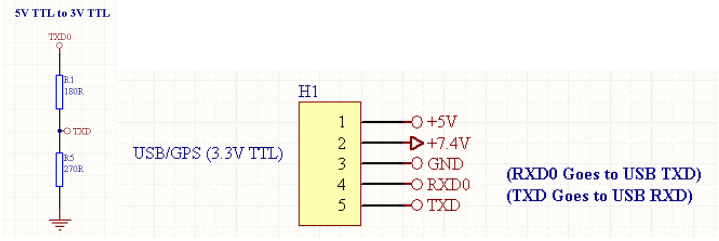

Figure 63: USB Connectivity

The Radio Control PPM Level Shifter was designed to connect directly to the RX Pulse Train I/O Connector (see figure 64). It formats the PPM signal from the transmitter into a level that can be easily read by the microcontroller (see figure 65). In the most basic principles it is simply a digital amplifier as the signal from the transmitter is between 0V and 1.5V which needs to be amplified to a range between 0V and 5V.

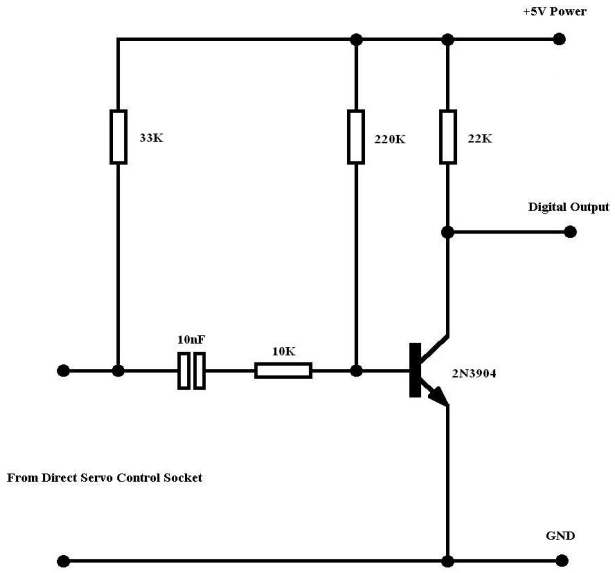

Figure 64: RX PPM Level Shifter

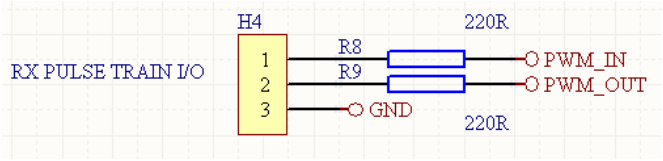

Figure 65: RX Pulse Train Connector

The Xbee radio network modem is connected to the microcontroller via a USART port. However the level fed into the Xbee needs to be limited to 3.3V so a simple voltage divider is used for level shifting (see figure 66). The values here are critical. If the resistance is too high then the digital response is to slow and cannot keep up with the baudrate. If the resistance is to low then the circuit consumes more power and the microcontroller may not be able to source the required current to change states.

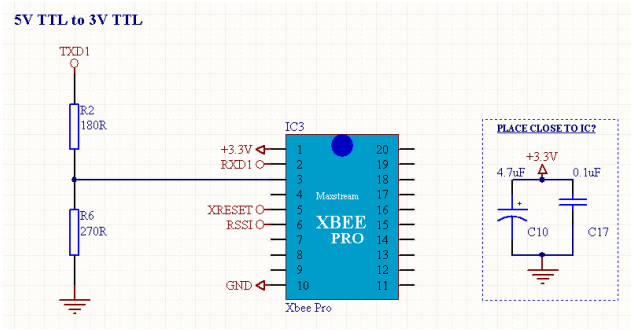

Figure 66: Xbee Radio Network Modem

The microcontroller is the heart of the circuit where all the devices in the circuit are connected in some way (see figure 67). This is where the PCB can become complex as many lines need to be routed in a tight space. The crystal oscillator provides the clock to the microcontroller at a frequency of 16 MHz.

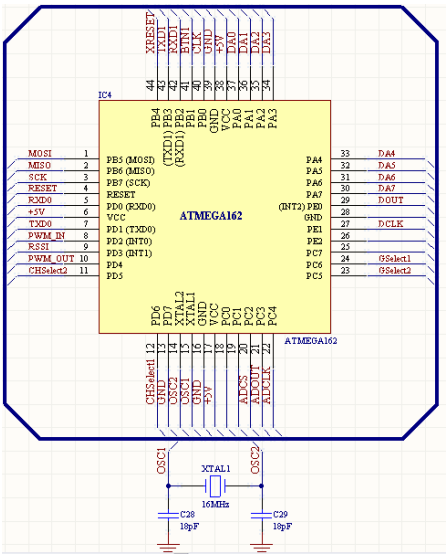

Figure 67: Microcontroller & Crystal Oscillator

The microcontroller is programmed via the SPI interface including the 'Reset' and power lines (see figure 68).

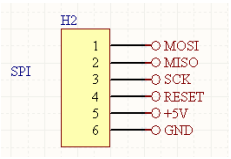

Figure 68: SPI Programming Socket

6.7.3 PCB Design:

Special anti noise and interference techniques need to be employed especially when designing a tight circuit with both analogue and digital circuitry in close proximity. The use of ground planes and strategic placement of parts is a critical part of the design process. It is important to place decoupling capacitors as close as possible to each and every integrated circuit. With this in mind the MicroBrain PCB was created in the

smallest most compact package incorporating sensors, processor & communications (see figures 69, 70 & 71).

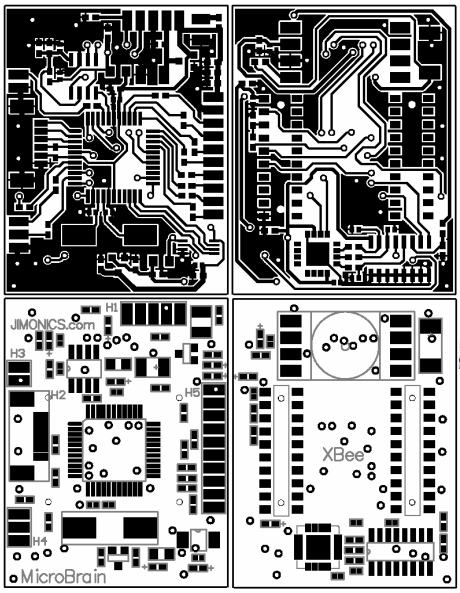

Figure 69: The MicroBrain PCB Layout (Not Actual Size)

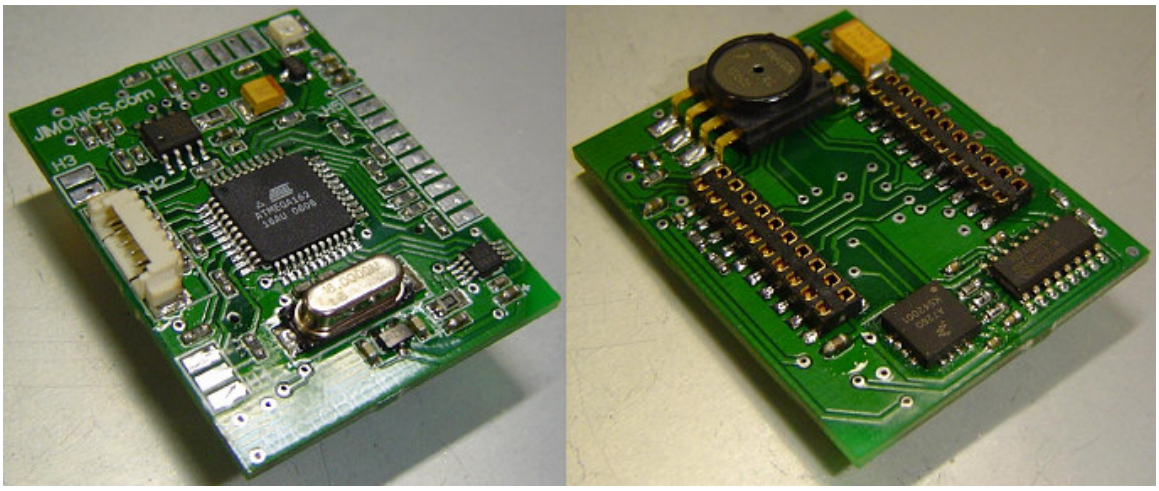

Figure 70: The MicroBrain Finished (45 mm x 35 mm) - Left: Top Layer, Right: Bottom Layer

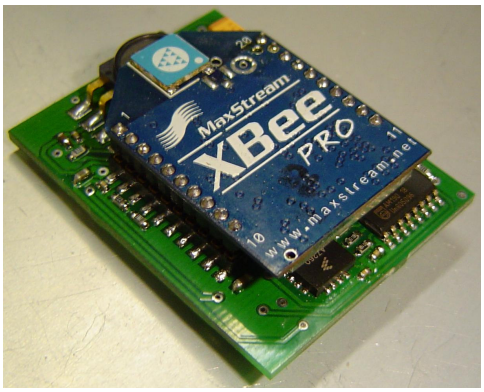

Figure 71: The MicroBrain Fitted With Xbee Radio Modem

6.8 External Sensor Connectivity:

The system has been designed to be the base autonomous platform for easy implementation of nature inspired sensors and algorithms. This section will discuss how the external sensors and/or processor can be connected to the system for easy implementation.

There are six serial peripheral interface (SPI) channels available for external sensor connectivity. Two of which are used for the 2-axis magnetometer, thus leaving four channels for external sensors. Each of these SPI channels could be used to connect to either an individual ADC or another processor. Data is transmitted in 8-bit bytes.

The 2-axis magnetometer is an example of an individual ADC connection where three lines are used for communication; serial clock, serial data and chip select. The serial clock and data lines are common to all devices. The chip select line is used to select

which device you wish to communicate with. A channel is read by first selecting its corresponding chip select line and then data is read in on the rising edge of the serial clock. The MicroBrain is the 'Master' and the external devices are the 'Slaves'.

If another processor is connected then a higher number of sensors could be implemented and the sensor data could be pre-processed for better computational efficiency utilising a distributed processing topology. This may be necessary if the guidance or navigational algorithm requires large amounts of computational power.

The typical application connectivity (see figures 72 & 73) shows two possible scenarios; individual ADC connectivity and processor expansion connectivity. Any combination between the two is permitted. The firmware of the MicroBrain would be coded depending on the required configuration and the actual implementation of the external sensors.

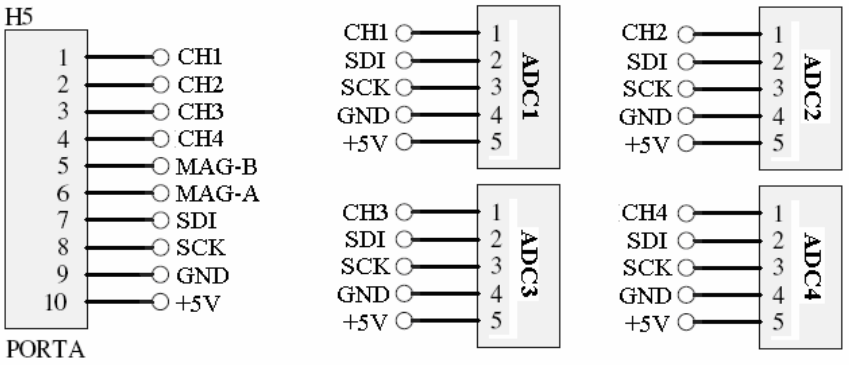

Figure 72: Individual Sensor Connectivity Using ADC's

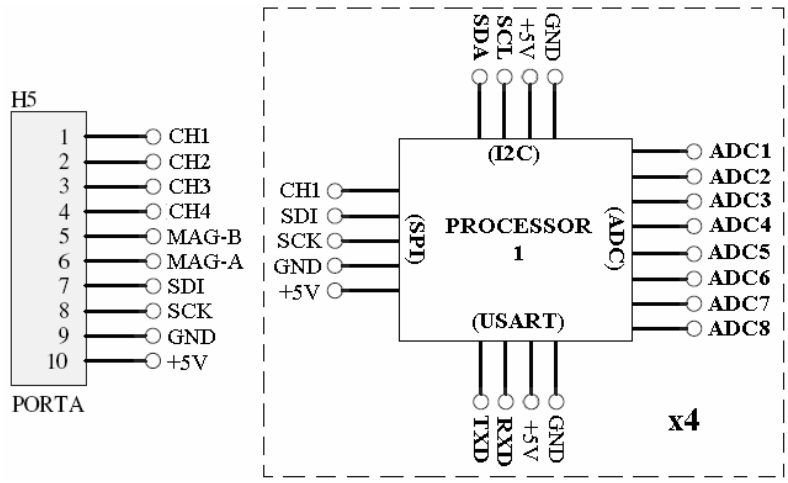

Figure 73: Multi-Processor Expansion Connectivity

When using the multi-processor expansion, control over the research flying platform is achieved by sending a set of four sequential command messages. These messages are ordered; Pitch, Roll, Yaw (Euler angles) and Altitude. 'The MicroBrain' will continuously send a sequence of low pulses to the CH1, CH2, CH3 and CH4 chip select lines at a rate of 100 Hz. This gives an individual update rate of 25 Hz for each channel. To tell 'The MicroBrain' that the device connected is another processor the channel line must be held low for 8 clock cycles after the initial low pulse. 'The MicroBrain then knows it will be receiving the four commands in the next 5 bytes of data. There are two bytes for the yaw bearing and one byte for each of the other command messages (Pitch, Roll and Altitude). These commands directly control the set points of their corresponding PID controller. The valid ranges for each are; Pitch – 0 to 180 (-45° to +45°), Roll – 0 to 180 (-45° to +45°), Yaw – 0 to 359 (0° to 359°), and Altitude – 0 to 255 (0m to +6.45m). The pitch and roll angles of the platform are limited naturally by the mechanical stabilisation.

Time ran out before full testing of this expansion connector was carried out, however, in theory everything should work as described, with minimal debugging required to achieve good robustness.

Chapter 7

7.0 Avionics Software Design:

There are three types of support software required to run the avionics hardware:

- The embedded flight computer firmware provides real time processing for;
    - Sensors
    - Controllers
    - Actuators

- The embedded ground station firmware provides real time processing for;
    - Remote control
    - Differential pressure updates
    - HMI sensor updates

- The ground station Human Machine Interface (HMI) allows for;
    - Graphical User Interface (GUI)
    - Displaying real time sensor data
    - Enabling higher level control

7.1 Embedded Flight Computer:

The embedded flight computer firmware is run on the ATMEGA162 onboard the MAV. The software is designed to; read the sensor information, compute & update the PID controller and send the required output to control the actuators. The update rate of this process is set to 100Hz. This frequency allows good control over the natural frequency of the platform.

7.1.1 Microcontroller Initialisation:

When the microcontroller powers up it first initialises itself. This involves:

1. Setting the device oscillator speed and watchdog timer
2. Setting the input and output directions of each port bit & pull-ups
3. Initialising the timers and counters
4. Setting the interrupt vectors
5. Initialising the serial communication
6. And loading the default variable and EEPROM values

7.1.2 Sensors:

Each of the sensors is read individually, filtered and the appropriate conversion is done to compute the desired format suitable for input into the controllers. This involves:

1. Reading the two heading 16-bit ADCs of the 2-axis magnetometer and computing the bearing
2. Reading the pressure sensor 24-bit ADC and computing the altitude
3. Reading the three axis accelerometer from the multiplexed 16-bit ADC and computing the Euler Angles.
4. Reading the system voltage divider from the multiplexed 16-bit ADC and computing the battery voltage.

7.1.3 Controllers:

The Proportional Integral Derivative (PID) controllers that were utilized were chosen mainly for their computational efficiency and good overall performance without detailed modelling of the platform dynamics. The block diagram below shows the basic PID configuration (see figure 74).

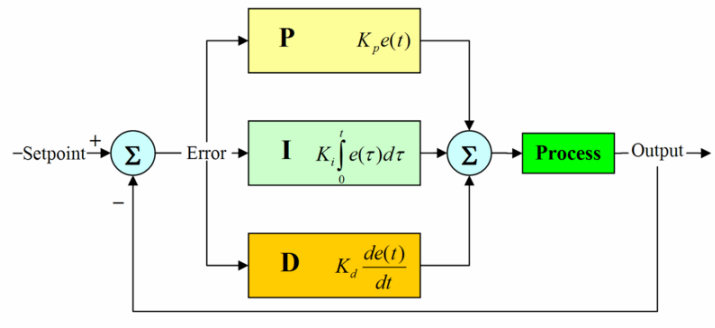

Figure 74: Basic PID Controller Block Diagram [37]

Attitude control of the platform is achieved using individual PID controllers, one for each of the four Degrees of Freedom (DOF); Roll, Pitch, Yaw and Altitude. The gains were tuned manually: first the Kp gain is tuned with Ki and Kd gains set to zero, then Kd is introduced to try and reduce the oscillation and improve the response, the Ki gain is then tuned to minimise the steady state error. The three accelerometer readings along with the two axis magnetometer readings are used directly to compute the 'measured' Euler Angles [50]:

Equation 10: Euler Angle - Roll

$$Roll = (atan2(\frac{ay}{g}, \frac{az}{g})) \times (\frac{180}{PI})$$

Equation 11: Euler Angle - Pitch

$$Pitch = (atan2(\frac{ax}{g}, \frac{az}{g})) \times (\frac{180}{PI})$$

$$where: \quad g = 9.8ms\text{-}2$$

Equation 12: Euler Angle - Yaw

$$Yaw = atan2(hX, hY) \times (\frac{180}{PI})$$

As there are no gyros data fusion is not necessary. The measured Euler angles should provide enough information to stabilise the platform, however, as the inclination angles are calculated by measuring pure accelerations, the platforms movement will disturb these readings. This raises the question - will this be good enough for fully autonomous control? The performance of this system will be evaluated in *Chapter 8*.

7.1.4 Actuators:

The output of the controllers is sent to the servo controller via one of the serial USART ports. The serial messages are then processed by the Jimonics SCM-18 servo controller to output the desired PWM signals enabling direct control of the pitch and roll servo positions, and the two motor speeds.

7.1.5 Main Program Flow:

The dataflow diagram showing how the previous sections are liked can be seen in the figure 75 below. It can be seen here that the five channels used to command the platform can either be sent from the radio modem, for manually guided autonomous mode, or from the external sensor inputs. The output to the top and bottom rotor motors are mixed together to control both altitude and yaw position.

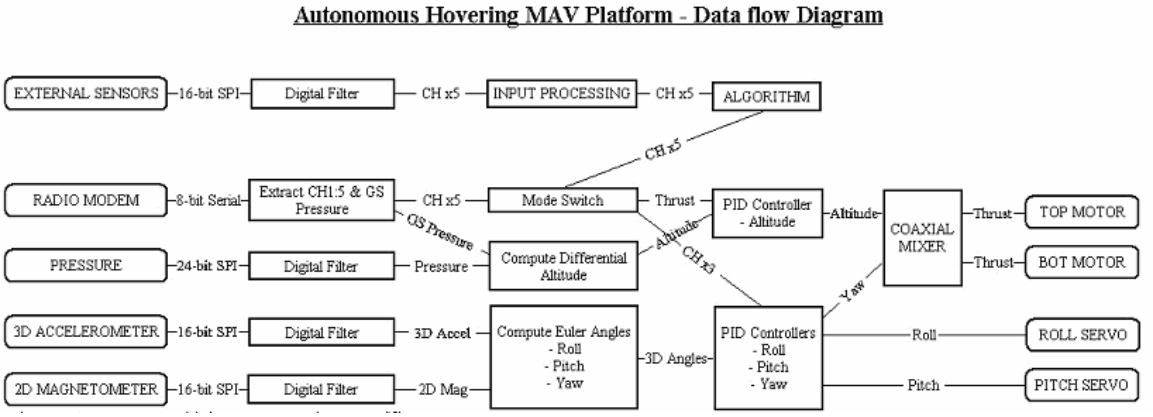

Figure 75: Embedded Flight Computer - Dataflow Diagram

7.2 Embedded Ground Station:

"The MicroBrain" was designed so that the same PCB can be used for both the platform flight computer as well as the ground station. This allows the embedded ground station firmware to be run on the generic "MicroBrain" board which has been configured for ground station operation.

7.2.1 Remote Control:

The embedded ground station is a real time processor that monitors the PPM signals from the manual R/C transmitter. The joystick positions are sent up to the platform via the radio modem to allow for full radio control and mode control manipulation. This is especially useful during the testing phase and during PID gain tuning, as you can change between manual modes and autonomous modes on the fly.

7.2.2 Differential Pressure Updates:

The ground station pressure is converted to an altitude and is then sent up to the platform and used for differential altitude control. Therefore the radio modem uplink messages incorporate both the manual joystick positions and the ground station altitude. The update rate has been selected to be 50Hz as this is the frequency that the remote control outputs joystick positions.

7.2.3 HMI Sensor Updates:

The ground station sends the received sensor information from the flying platform to the serial port connected to a Personal Computer (PC). This connection is provided by a USB cable which has a built in USB to serial chip which can be soldered directly to the PCB. The USB cable also provides power to the ground station thus eliminating the need for extra batteries.

7.2.4 Main Program Flow:

The embedded ground station data flow diagram below shows the interconnectivity between the; R/C transmitter, PC and radio modem (see figure 76).

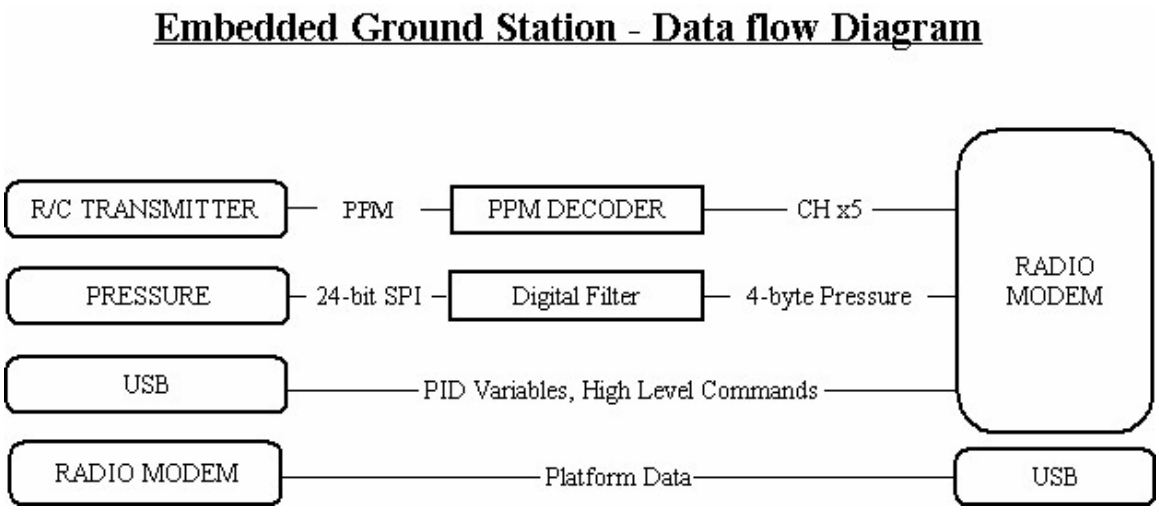

Figure 76: Embedded Ground Station - Data flow Diagram

7.3 Ground Station HMI:

The ground station HMI software is run on either a PC or Laptop Windows machine. The application interface is used to display the real time information from the platform and the ground station (figure 77).

7.3.1 Graphical User Interface (GUI):

The GUI, written in Visual Basic, provides an easy way of viewing the real-time sensor data from both the flying platform and the ground station. The GUI also provides a way to log this data to a file so the information can be analysed post flight. The GUI colours and layout are important as they interface the user with the system. The user must be able to interpret the data in the most natural way. By breaking the layout into appropriate sub sections and formats it makes the data easier to read.

7.3.2 Displaying Real-time Sensor Data:

The ground station sensor information includes; raw ADC pressure data, ground pressure (kPa) and altitude above sea level.

The airframe sensor information includes; raw ADC pressure data, aircraft pressure (kPa), differential altitude (m), aircraft bearing (deg + compass), X, Y & Z raw ADC data and X, Y, & Z accelerations (g).

The controller variable information includes kp, ki & kd gains for each PID controller; altitude, X-axis & Y-axis and Yaw. The current gains can be requested, adjusted and uploaded to the aircraft on the fly. The trims of each can also be changed by moving the corresponding slider. The PID controllers can individually be activated or deactivated depending on the level of autonomy required. This is especially useful during the PID gain tuning as you can change the PID gains of different PID feedback loops and test them individually.

The other information displayed includes; radio modem signal strength, current link rate, battery health and the current mode.

7.3.3 Configurable High-Level Control:

The interface was also envisioned to have the capability of implementing various different control functions depending on the experiment at hand. This part of the GUI (lower right – figure 77) could be configurable to allow the user to specify what information they would like to display or to allow for control over specific parameters.

In figure 77 an example of a conventional waypoint controller has been created, where a simple sequence of tasks could be commanded based on velocity and time. This part of the interface was of secondary priority, as it is not directly related to the goals of the project, so only the base system has been established however it is ready for adding full functionality.

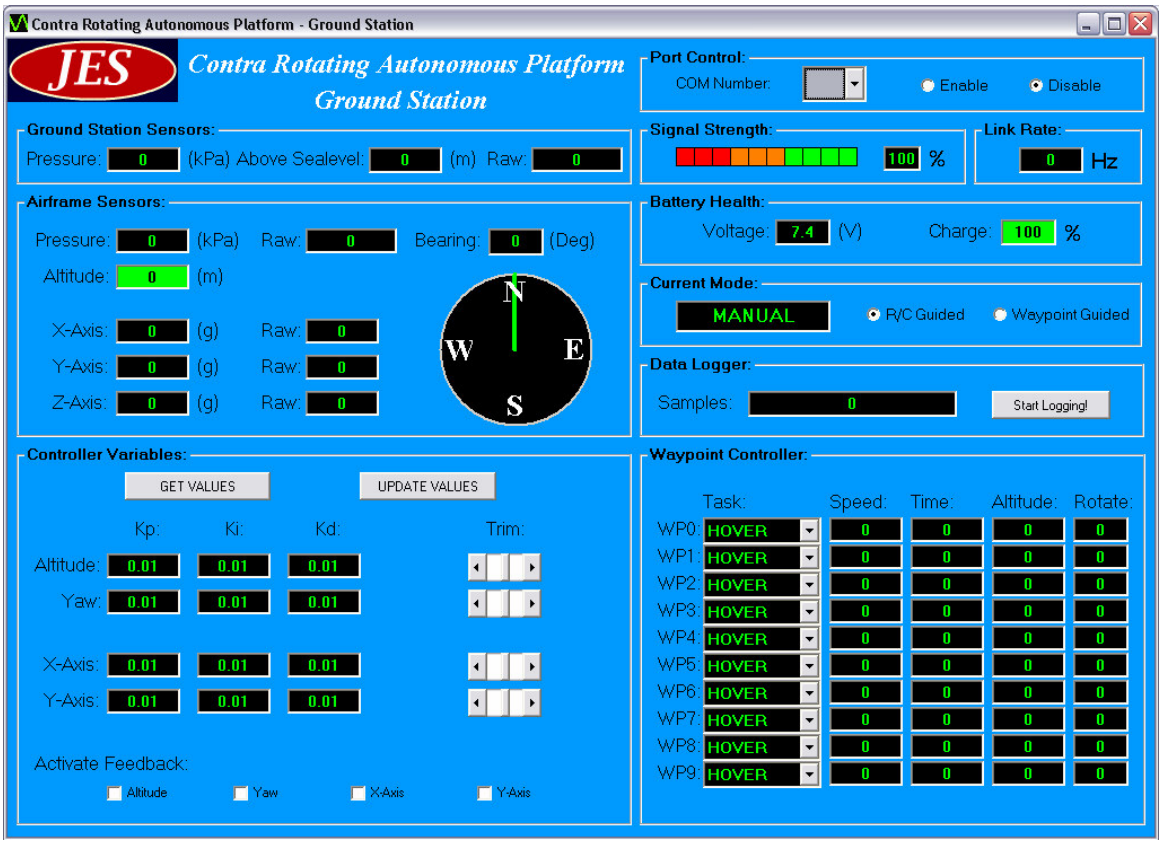

Figure 77: Ground Station HMI - Screen Shot

Chapter 8

8.0 Operational Testing:

The operational testing stage is where the hardware, firmware and software are integrated together and tested. Many of the problems involved with integration are due to the discrepancies between the initial design idea and the limitations of the actual hardware and/or software. These are not usually discovered until the hardware, firmware and software are tested together. The method used for integration was a segmentation process with many individual sub testing stages of modular functions. By breaking up the design into modular segments we are able to test the performance and tune them to make integration easier.

Firstly the performance of each sensor was tested by writing the support firmware for interfacing the sensor to the microcontroller and storing the data from the ADC into a variable. Lower level modular functions were then developed to convert the ADC values to a meaningful format e.g. the two 16-bit ADC values from the magnetometer get converted to a yaw bearing. This information was then displayed on an LCD screen to prove that the information was true and accurate. Once the sensor information was considered accurate then the performance was tested by creating a test rig or experiment. These experiments were developed to prove that the sensor could be implemented into the final design as initially intended.

8.1 Sensor Testing:

8.1.1 MEMS 3D Accelerometer:

Method:

The 3D Accelerometer sensor board was tested by writing the code to read the three 16-bit ADC values from the SPI bus and then converting the data to 'G's'. The acceleration was then displayed on the LCD screen. These accelerations were then used to calculate Euler Angles and were displayed on the screen.

Problems:

There were some problems with displaying a floating point number with five decimal places on the LCD screen as the conversion from a float to individual characters was not available in any of the standard C libraries. Note that at this time the GUI interface was not yet completed.

Solutions

A set of LCD functions were created to be able to display any type of number including floating points. This was done by testing the data type and then simply shifting the decimal point by doing basic division and addition, to segment out individual numbers. The process is computationally expensive however it is only needed while testing and when only one sensor is being tested there is more than adequate processing power.

Performance:

The sensor provided a nice fast response (50Hz) and an accurate resolution (~0.017 g).

8.1.2 2-Axis Magnetometer:

Method:

The 2-axis magnetometer sensor board was tested by writing the code to read the two 16-bit ADC values from the SPI bus and then converting the data to a bearing. The bearing was then displayed on the LCD screen. Code was then created to test the automatic yaw control implemented with a PID controller. The coaxial platform was placed on a ¼ inch bearing which allowed the platform to rotate with minimal friction. The set-point for the controller was 180°. (***See "Bearing Test" video***)

Problems:

There were some problems with calibration. If the calibration was not accurate then the whole 360° range could not be achieved. When placed near metal the sensor output was grossly distorted e.g. motors or gyroscopic bar.

Solutions

A calibration function was created to find the origin of the two sensors. This was achieved by recording the maximum and minimum values read by the ADC as the sensor was rotated the full 360°. These values were then divided by two to find the origin.

Performance:

The sensor provided an impressive and fast response (better than 100Hz) with very accurate readings (~0.1°). When used on the platform the controlled bearing was within ±3° (as seen in the video). The small fluctuation could be due to the controller response

or may be an effect created by the EM interference fields of the two electric motors. A major draw back was when the sensor was not exactly flat the bearing was skewed by a few degrees depending on the inclination angle. However, this could be minimised by using the pitch and roll Euler angles for inclination vs. bearing correction. This could also be influencing the yaw bearing fluctuations if the tail was not perfectly flat while rotating.

8.1.3 Pressure Altitude:

Method:

The pressure altitude sensor was tested by developing an altitude hold autopilot that consisted of a custom built altimeter and PID controller, fitted to a foam toy UFO shell (see figure 78). The original electronics, motor and batteries were replaced with custom avionics, higher power motor and LIPO cells respectively. Once the system was turned on it is held up to the altitude in which you would like to calibrate to. The system is then placed on the ground and will autonomously fly back up and hover at the calibrated altitude. (***See "Altitude Hold Autopilot" video***)

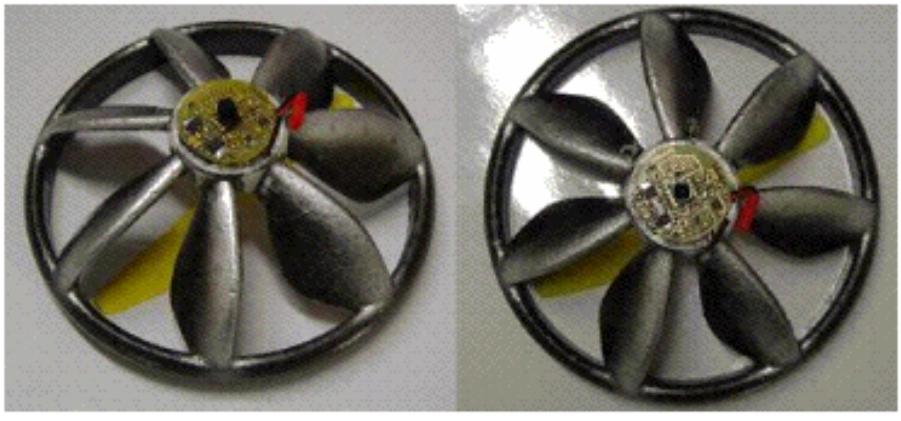

Figure 78: Altitude Hold Autopilot

Below are the results of two tests conducted to test the linear relationship of pressure with measured altitude. The tests were conducted in a stairwell over seven levels. The tests show the output before and after calibration (see figures 79 & 80).

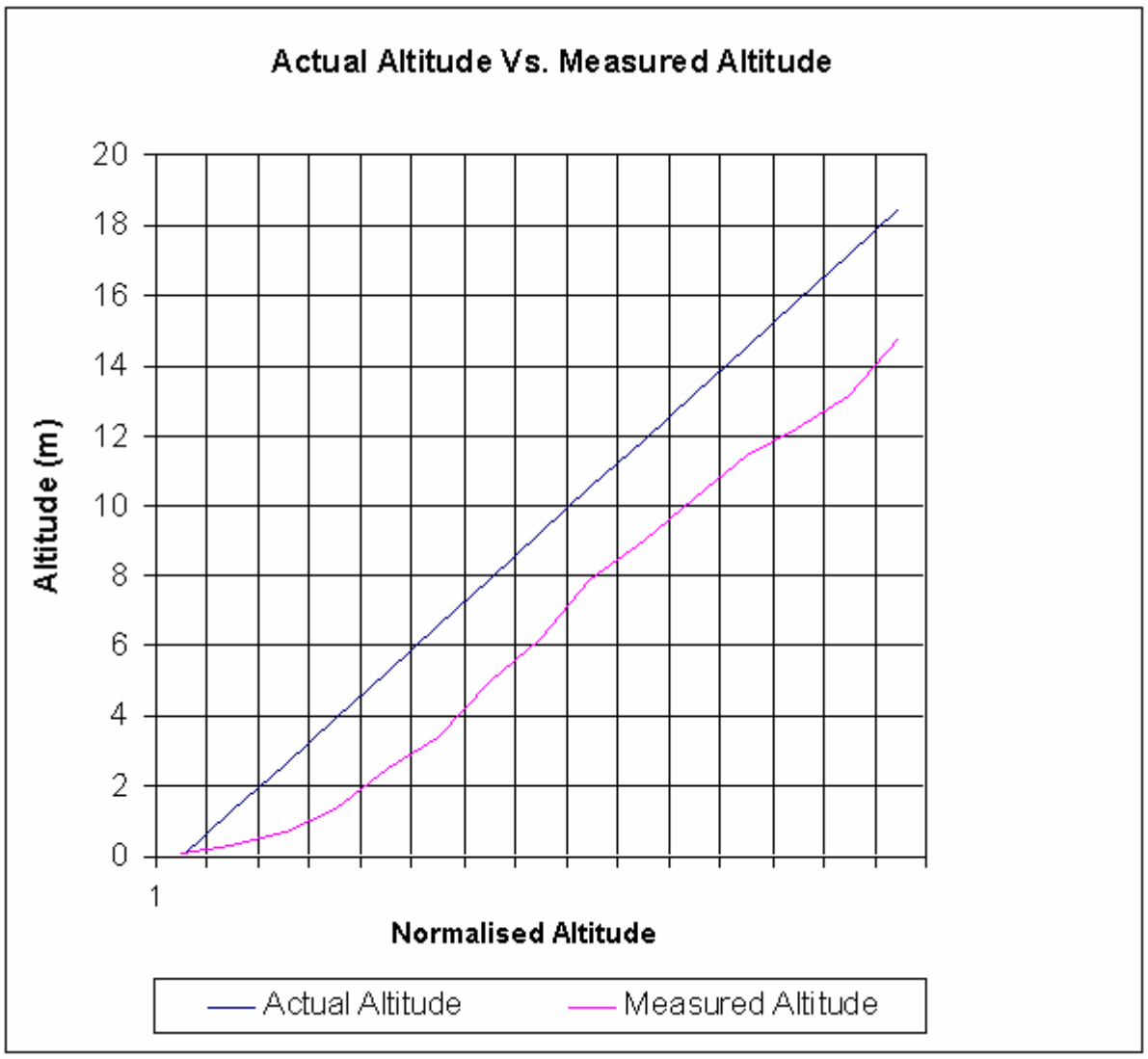

Figure 79: Altitude Test – Before Calibration

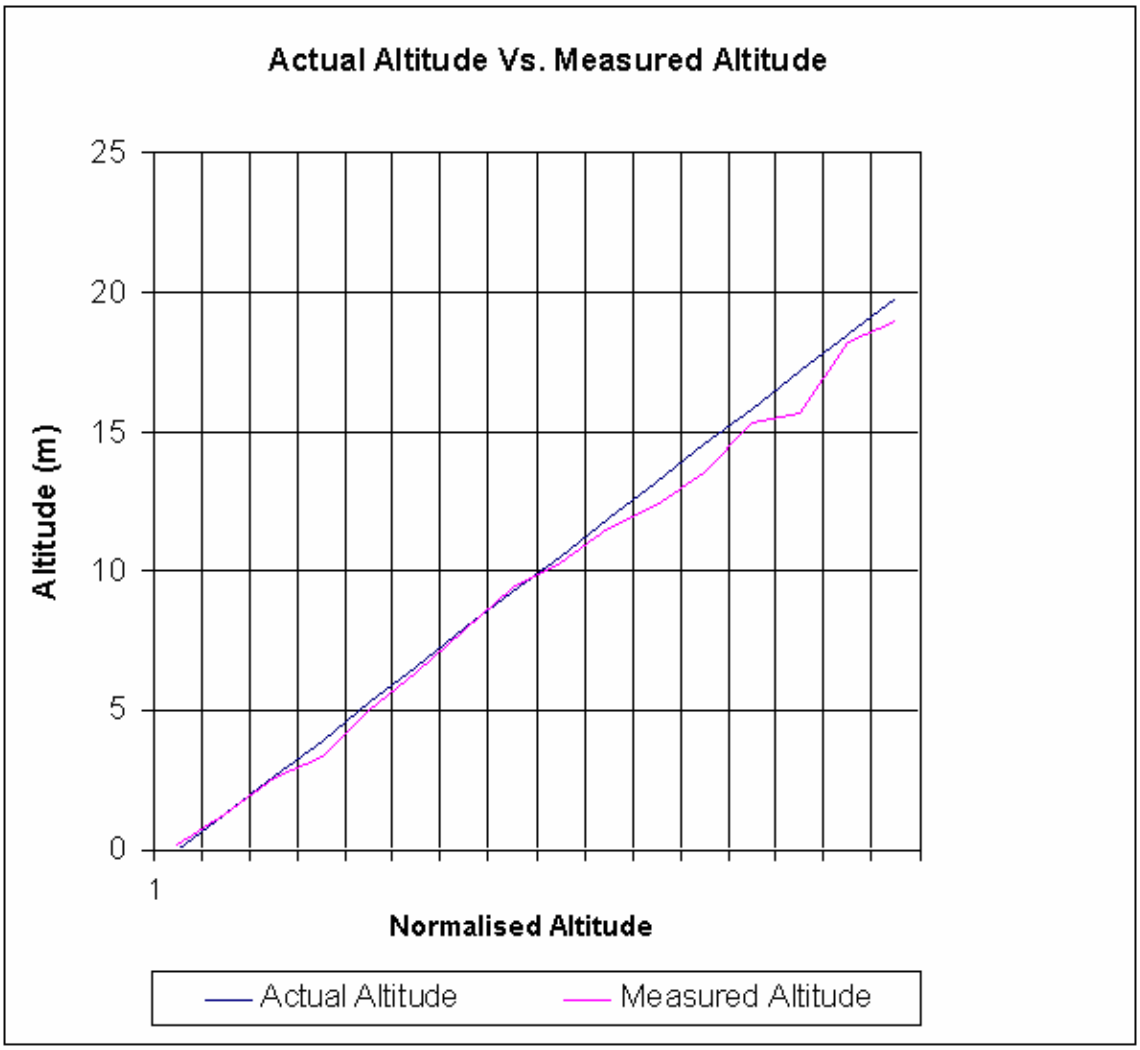

Figure 80: Altitude Test – After calibration

By using a simple interpolation method calculated from the slope, you can achieve a good result over a large range of altitudes without having to compute the standard atmospheric altitude equations. Sixteen ranges were used to minimize the computational requirement when running the code on a microcontroller (see figure 81).

RANGE (m):	TEMP (C):	PRESSURE (Pa):	DENSITY (Kg/m^3):	DELTA (Pa):	SLOPE (Pa/m):
-1000	21.5	113929.0831	1.347		
				12604.0831	12.6040831
0	15	101325	1.225		
				11450.4295	11.4504295
1000	8.5	89874.5705	1.1116		
				10379.355	10.379355
2000	2	79495.2155	1.0065		
				9386.6708	9.3866708
3000	-4.5	70108.5447	0.9091		
				8468.3094	8.4683094
4000	-11	61640.2353	0.8191		
				7620.3232	7.6203232
5000	-17.5	54019.9121	0.7361		
				6838.8845	6.8388845
6000	-24	47181.0276	0.6597		
				6120.2844	6.1202844
7000	-30.5	41060.7432	0.5895		
				5460.9318	5.4609318
8000	-37	35599.8114	0.5252		
				4857.353	4.857353
9000	-43.5	30742.4584	0.4663		
				4306.1908	4.3061908
10000	-50	26436.2676	0.4127		
				3804.2036	3.8042036
11000	-56.5	22632.064	0.3639		
				3301.659	3.301659
12000	-56.5	19330.405	0.3108		
				2819.9992	2.8199992
13000	-56.5	16510.4058	0.2655		
				2408.6062	2.4086062
14000	-56.5	14101.7996	0.2268		
				2057.2287	2.0572287
15000	-56.5	12044.5709	0.1937		

Figure 81: Sixteen Pressure Altitude Ranges

Problems:

There were some initial problems with obtaining a good constant altitude measurement. Within minutes fluctuations in pressure would occur that moved the calibrated value depending on the weather and time of day.

Solutions

Extensive research was done to find the best referencing and filtering techniques to achieve high resolution. The chosen version uses a 24-bit ADC to maximize results. A differential pressure system was developed to prevent fluctuations, as the fluctuations would be consistent over both sensors. The difference between the two sensors is used to calculate the altitude. Also temperature and humidity corrections can be used to increase the accuracy, with large changes in atmospheric conditions like rain, sunshine and high humidity.

Performance:

The sensor performance was quite good giving an accuracy of ~10cm and a resolution of ~5cm. This novel idea proved to be of great benefit in simplifying the difficult task of altitude control.

8.2 Platform R/C Testing:

The platform's flight characteristics and performance was tested using a 6-CH JR transmitter (see figure 82). The Direct Servo Connection (DSC) provided the PPM signals to the embedded ground station where the signals are decoded and sent up to the platform via the Xbee Radio Modems. The first four channels are used to control the Throttle, Roll, Pitch and Yaw which are linearly proportional to the servo and throttle commands. The fifth channel is used to switch between manual and autonomous modes which are physically controlled by a toggle switch on the top right hand side of the remote. The sixth channel was unused. When using the DSC, the power transmitter inside turns off and thus consumes less power.

Figure 82: JR Radio Control Transmitter [51]

8.2.1 Collision Protection System:

Method:

In order to test the collision protection system we first needed to make sure the R/C manual controls (up-link) were robust. Once this was determined, by range testing and debugging, the platform was flown in manual mode and commanded to fly into a wall. The platform was then commanded to fly into the ceiling. A video of this test has been documented. (***See "Collision Test" video***) The idea of this test was to understand the robustness of the structure, and the fall-back, manual mode up link, which is vital during the testing/tuning stage.

8.2.2 Test Results:

The results showed that the structure was well designed and the collision protection system was a success. The manual mode control proved to work well at 50Hz (20ms delay) and showed good robustness and reliability.

8.2.3 Problems:

The collision protection system will only work on flat surfaces without protruding objects due to the open cage design. When the switch mode power supply of the laptop was plugged into the mains supply, the noise generated by the switching regulator disrupted the delicate reading of the DSC PPM signal.

8.2.4 Solutions:

The collision protection system cage could incorporate more vertical rods and thus block smaller objects. The power supply was disconnected during the flight tests to prevent disruptions of the DSC PPM signal reading.

8.3 Yaw Control Testing:

Method:

The performance of the yaw controller was tested by implementing the yaw PID controller on its own. Once the pilot switches to Autonomous mode the throttle, roll & pitch are controlled remotely by the pilot, and the yaw controller controls the heading of the platform autonomously. The heading hold yaw controller was first tested on the ground by pre-programming the initial heading in degrees and manually increasing the throttle to make the platform light on its feet. Thus allowing the differential throttle to alter the heading autonomously. The heading hold yaw controller was then tested in flight.

8.3.1 Test Results:

The performance of the heading hold system, without the use of a rate gyro, was quite good. The accuracy was within ±3°, comparable to the bench test results. There was a quick response with minimal overshoot. (S***ee "Autonomous Heading Hold" video***)

8.3.2 Problems:

The 2-axis magnetometer had a tendency to give slight errors in the heading when the attitude of the platform changed. If the platform was dead flat, the performance was flawless. If the platform had a slight pitch or roll then the heading would be skewed depending on the inclination angle. This can be seen in the video.

8.3.3 Solutions:

The pitch and roll angles from the Euler angles could be used to correct this skewing of the heading as they are proportionally related.

8.4 Roll & Pitch Control Testing:

Method:

The performance of the Roll and Pitch controller was tested by implementing the roll and pitch PID controllers on their own. Once the pilot switches to Autonomous mode the throttle & yaw are controlled remotely by the pilot. The roll & pitch controllers then control the roll and pitch of the platform autonomously. The roll and pitch Euler Angles were used as the input to two separate PID controllers. The roll and pitch commands given by the pilot were directly controlling the set points of the PID controller.

8.4.1 Test Results:

The attitude hold system seemed to perform well. The platform needed minimal corrections for the X and Y positions. (***See video in next section***)

8.4.2 Problems:

Attitude control is an extremely difficult task, as the inaccuracies of the cheap MEMS sensors cause a drift over time. This drift will continue to get larger unless it is corrected. With an indoor platform the complexity increases as you cannot use a GPS to correct the position. You can see, in the video, this drift over time as the platform slowly goes off in a random direction. The mechanical stabilisation system induces a slow oscillation.

8.4.3 Solutions:

The drift error of the system could be reduced by using higher quality MEMS sensors. Also position corrections could be implemented using a defined reference from another sensor such as an ultrasonic sensor directed at a wall.

8.5 Full Autonomy Testing:

Method:

The performance of the Roll, Pitch and Yaw controllers was tested by implementing all of the PID controllers. Once the pilot switches to Autonomous mode the throttle command is controlled remotely by the pilot. The roll, pitch and yaw controllers then control the roll, pitch and yaw of the platform autonomously. The roll, pitch and yaw Euler angles were used as the input to the three separate PID controllers. The throttle, roll, pitch and yaw commands given by the pilot were directly controlling the set points of the PID controllers.

8.5.1 Test Results:

The performance of the fully autonomous hovering system was quite good. The platform needed minimal corrections for the altitude. X, Y and Yaw corrections were not required. (***See "Full Autonomy" video***)

8.5.2 Problems:

The platform drifted slowly in a random direction due to the inaccuracies described previously. Unfortunately differential altitude corrections were not implemented as time ran out to complete the project.

8.5.3 Solutions:

As stated previously the drift could be minimized by obtaining more accurate inertial sensors, or by implementing an X & Y referencing correction system. Altitude corrections have been proven in the sensor testing and would be expected to perform well.

Chapter 9

9.0 Example Application:

This chapter is designed to show how easy the research flying platform is to use. This is an example application that is aimed at creating a research project for a group of three or four students. This brief example is intended to give the teacher some key ideas for starting a project using the research flying platform.

NOTE: A relatively good understanding about basic electronics, microcontrollers and writing C code is assumed knowledge in this example. It is intended to give a brief overview only.

9.1 Project Description:

The aim to this project is to create a flying robot that can autonomously fly down a corridor by implementing a simple collision avoidance algorithm. Biologically inspired sensors will be used to detect objects. Fruit bats (see figure 83) and dolphins (see figure 84) use a technique called sonar to detect food and objects in their natural environment.

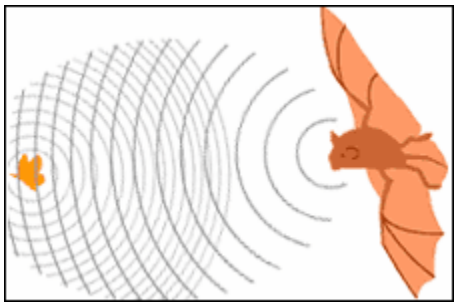

Figure 83: Fruit Bat Using Sonar [52]

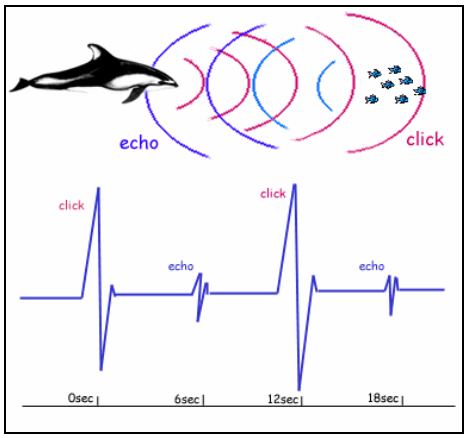

Figure 84: Dolphin Using Sonar [53]

In this project sonar will be used to simply detect the distance to an object. The sonar device transmits a high frequency in-audible (to humans) sound into the environment, typically 42 kHz, and then listens for the reflections. To determine the distance to an object, all that is required is the measured time of flight and the speed of sound. Therefore the distance is simply the speed of sound multiplied by half the time of flight (see equation 13).

Equation 13: Sonar Distance

$$Distance = \frac{(Speed\ of\ Sound \times Time\ of\ Flight)}{2}$$

The external hardware will consist of three ultrasonic range sensors utilising this technology and a small microcontroller. Two of the ultrasonic range sensors will measure the distance at an angle +45° and -45° respectively, in front of the platform. And the third will measure the distance to the ground. The microcontroller will read the distances, compute the algorithm and send the appropriate commands to the flying platform to control the direction the robot is flying.

9.2 Recommended Hardware:

The hardware could consist of three ultrasonic sensors connected to an ATTINY26 (ATMEL) microcontroller. The microcontroller can be connected to the research platforms external sensor SPI interface with five wires; power (+5V), ground (GND), serial clock (SCK), serial data (SDI) and chip select (CH1). The power lines are also connected to each of the sonar sensors. The microcontroller is connected to an external 16 MHz crystal resonator that will run the microcontroller at 16 MIPS. This will provide more than enough processing power for this project (see figure 85). The programming port can be connected directly to an ISPAVRU1 programmer [54].

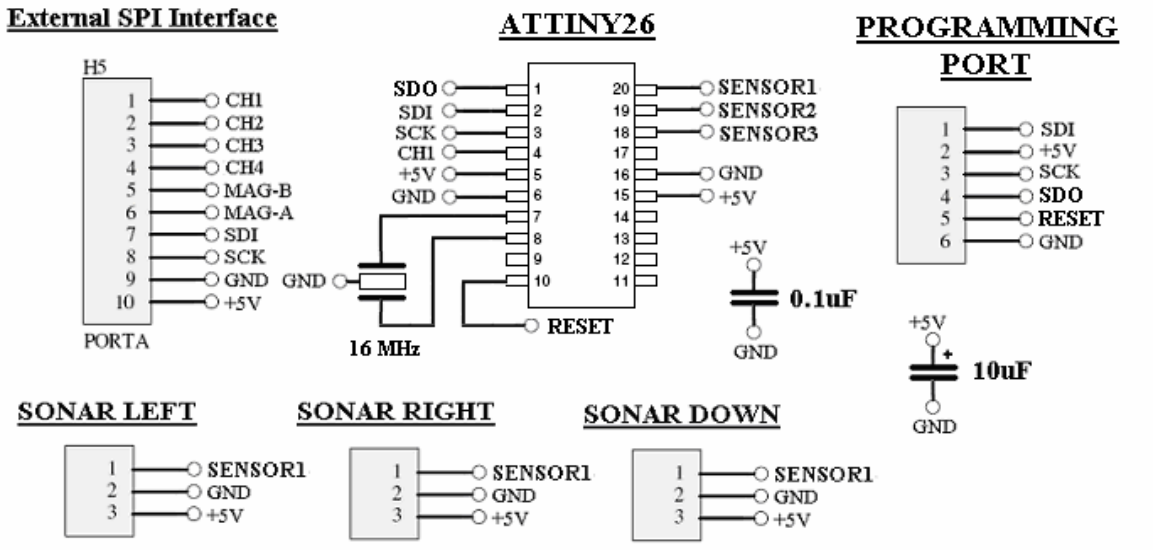

Figure 85: External Sonar Sensor Schematic

9.3 Method for Calculating Distance:

Three LV-MaxSonar®-EZ1™ [55] ultrasonic sensors (see figure 86) will be used in this experiment to provide the feedback for autonomous collision avoidance. The sensors weigh 4.3 grams each and have a range from 1 to 255 Inches (6.45m). The sensors can output in three different formats; serial, pulse width modulation and analogue voltage. The format used in this experiment will be the analogue voltage output where 10mV represents one inch. Only three connections are required for each sensor; +V, GND and analogue output.

Figure 86: LV-MaxSonar®-EZ1™ [55]

The built in 10-bit analogue to digital converter (ADC) of the microcontroller will be used to measure the output voltages of each of the three sensors. The sensors are connected to ADC0 (pin-20), ADC1 (pin-19) and ADC18 (pin-2) (see figure 87).

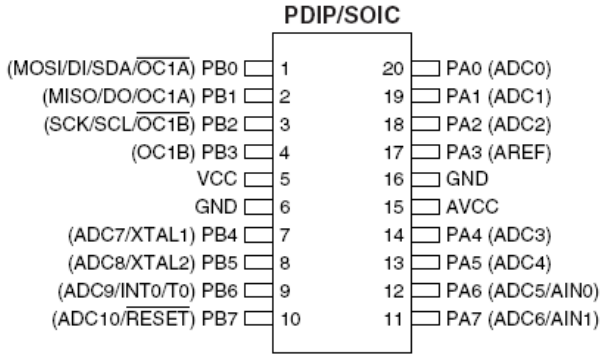

Figure 87: ATTINY26 Microcontroller Pin-out

The internal ADC channels will be read sequentially and placed into three variables representing the three ADC readings. An interrupt will be generated after each conversion to trigger the distance calculation. The following equation can be used to calculate the distance (see equation 14).

Equation 14: Distance from ADC Value

$$Distance = (ADC \times 0.48828125)$$

9.4 Implementing a Collision Avoidance Algorithm:

The platform can be commanded to have a slow constant forward pitch and a static roll & altitude. The altitude can be corrected using the downward facing sonar sensor. A simple collision avoidance algorithm can be used to simply adjust the yaw of the flying platform as the vehicle fly's forward. As the flying platform approaches a wall on its left, the algorithm could adjust the yaw so that the flying platform is turned away from the obstacle, in this case to the right. A simple 'if' statement could be used to determine if both distances are smaller than a pre-defined threshold. This could then trigger an action such as a 180° turn to prevent a head-on collision. Many interesting behaviors could be programmed and tested by the students.

9.5 Auto Generation of the Structure of the Main Program:

The microcontroller code will be in C using the Code Vision compiler [56] and programmed with the ISPAVRU1 programmer. The Code Vision compiler has a built in wizard that will aid in the setup of the main program loop and basic initialisation. When using the wizard, select the 16 MHz clock speed and then set the SENSOR1, SENSOR2, SENSOR3, SDO and CH1 pins as inputs. Then select the SDI pin as an output. Make sure the SPI interface is enabled and the ADC on each sensor pin is enabled. Enable the external interrupt on the CH1 pin. After selecting the appropriate initialisation the wizard then will then create the initialisation code and the main program loop. Use the built in C libraries for the SPI (USI) and ADC communication. The program is then ready for coding the distance calculation and the collision avoidance algorithm. To autonomously control the flying platform using the SPI interface send the four higher level commands (Pitch, Roll, Yaw and Altitude) as discussed in the External Sensor Connectivity section (6.8). 'The MicroBrain' will send a trigger on the CH1 pin. This external interrupt is intended to be used to start the command message transfer to the flying platform.

9.6 Possible Sensor Placement:

The three sonar sensors need to be placed strategically to get the maximum performance of the project. The sensors can be placed at any point around the perimeter, top and bottom of the cage. For this experiment it would be necessary to place two sonar sensors towards the front at an angle of +45° & -45° respectively. The other sonar sensor can be placed on the bottom-front of the cage facing down (see figure 88). Note that the extra weight at the front would need to be balanced by sliding the battery backwards.

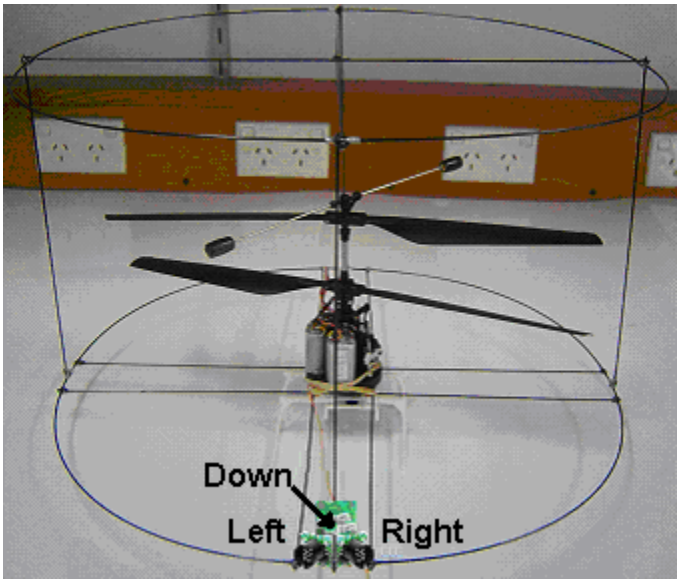

Figure 88: Placement of the Left, Right and Downward Facing Sonar Sensors

9.7 Recommended Analysis:

The students could then analyse the performance of their autonomous flying robot by logging the data from all the sensors using the application software provided (section 7.3). The students could then optimise their algorithm for best performance. Different thresholds, sonar angles, triggers (maybe a random change of direction trigger) could be implemented and tested. The system performance could also be tested in different environments.

Chapter 10

10.0 Closing Remarks:

The task of creating an autonomous flying platform is not a trivial one. The success of this project has been heavily dependant on the choices made from the preliminary research. This study was aimed at providing a realistic view on the current technologies and allowing for a practical conclusion based, not only on theoretical research, but also on practical experimentation.

10.1 Discussion:

The collision protection system is one of the most practical and useful devices that could be implemented on this type of hovering system. It has proven in many cases to be a "life saver" when things have gone wrong, especially during the initial stages of the PID gain tuning. It allows you to be more aggressive with what you try without having to worry too much about totally destroying your platform. The collision protection system has protected the platform during a fall from two floors onto a concrete without any damages. However it does not mean it is invincible. Its major vulnerability is if an object enters from one of the four quadrants and touches the blades, the reasoning is quite obvious. The collision protection system is designed primarily for flat walls with no protruding objects.

The major limitation to this platform is endurance. The intended goal endurance of ten minutes was however met. While this timeframe is often long enough to view and record

the performance of a single set of external sensors and algorithms if you were implementing a swarming system or evolutionary system this may not be sufficient. For these areas of research it is suggested that the researcher do as much as possible in simulation before transferring to the practical system. This limitation is governed by the energy density of the best available battery technology. Until the battery industry releases higher performance cells, or an alternate energy source is considered, we are stuck with this limitation.

The measured Euler Angles were not quite as accurate as they could have been. The gravity component calculation used to calculate the Euler angles was wrong. This was discovered after the testing phase was completed. The correct definition that should have been used as a substitute for relative gravity is as follows:

Equation 15: Euler Angle – Gravity Component

$$g = \sqrt{(ax \cdot ax + ay \cdot ay + az \cdot az)}$$

This calculates the summed gravity component from each axis as it changes depending on the attitude of the platform. By implementing this correction it is believed that the attitude stability would perform significantly better and may have reduced the slow oscillations during fully autonomous flight.

10.2 Future Work:

The following four points would be a recommendation to improve the overall performance of the autonomous system:

1. The differential altitude sensor was not active during the full functionally testing. The hardware has been designed to support this feature. However to get this feature to correct the change in altitude, the firmware for the 24-bit ADC driver would be required. By activating the differential altitude corrections there would be no need for manual corrections as seen in the video.

2. The radio modems were used to send the manual controls to the aircraft. As this requires a fairly high bandwidth when converting the signals to ASCII and transmitting them at 50Hz (defined by the R/C PPM signals) there was minimal overhead for sending other data. This was the main reason for minimal flight test logging. Manual control could be implemented by integrating a receiver circuit into the onboard avionics. This would allow the full bandwidth of the radio modems for data transfer and logging.

3. By integrating the PCB with the propulsion system structure the weight could further be reduced to allow for a longer endurance and/or increased payload.

4. A brushless motor conversion would increase the propulsion system efficiency, thus increasing the flight time and payload capacity of the platform.

10.3 Conclusion:

There are an increasing number of reasons for entering dangerous and cluttered indoor environments to do search and rescue type missions. Scientists are looking to nature for the answers to difficult guidance and navigation problems, however the implementation process is often limited to simulation. By using a flying platform, together with these algorithms and sensors, it could be possible to increase the efficiency and achieve higher level mission complexity. A broad range of expert knowledge is required to develop a platform capable of implementing such algorithms. This is often knowledge the typical scientist is not accustomed to.

Using the information within this thesis an autonomous flying platform could be manufactured that is specifically designed to allow scientists to test their novel sensors and algorithms. To implement their experiment it is possible that all a scientist may have to do is simply unpack the flying platform straight from the box, plug in their external sensors and upload their algorithm.

The research in the state of the art revealed that:

- Carbon fibre was the best material to use for the structure as it is light weight and incredibly strong.
- The best propulsion system would be the combination of brushless motors and lithium polymer batteries however this was not used due to the required structural changes involved.

- The minimal approach to obtain measured Euler Angles using only a 3-axis accelerometer and a 2-axis magnetometer worked, however, it is not an optimal solution.
- Altitude was measured accurately (~5→10cm) using air pressure.
- All the processing was done with a single high end ATMEL microcontroller.

Research in the state of the art platforms showed that:

- The most suitable platform was a coaxial contra-rotating helicopter with a semi-articulated gyroscopic stabilizer bar and cyclic translational control.
- The inherent stability of a platform can be used to make autonomous control easier, however, the system introduces a slow oscillation possibly due to the gyroscopic effects.
- There was a direct compromise between stability and controllability. The platform that was chosen traded off more stability for a reduction in controllability.
- There was a direct compromise between payload and flight time.

Sensor testing revealed that:

- Due to the neutrally mechanically stable system there is no real need for gyro sensors however they will improve the performance slightly. The best way to test the sensors was to design experiments to individually analyse the performance before integrating with the final design.

- Integration was best done by understanding how the system control was coupled to individual sensors or groups of sensors and implementing those singularities separately.

External sensors could be mounted by:

- A light weight carbon fibre 360° mounting system that doubles as a collision protection system.

Processing power capability:

- A high end microcontroller running at 16MIPS has enough processing power to; read all the onboard sensors, compute the PID control for a 4-DOF system, and output commands to actuators and motors. This was done at a system refresh rate of 100Hz.

PCB integration:

- It is possible to incorporate the entire avionics on a single double sided PCB. Except for the magnetometer which needs to be placed as far away as possible (>20cm) from any ferrous materials or magnetic fields caused by motors.

Safe testing was achieved by:

- Developing a collision protection system capable of withstanding small collisions with no problems. This means you can be more aggressive with your PID tuning and testing as minor crashes are not a problem, thus promoting a rapid development time.

Numerous autonomous flights were achieved which gave an insight into a new type of hovering system that requires minimal sensors for fully autonomous control. The overall project has proven to be a great success. This system eliminates the need for scientists and engineers to develop a testing platform. In doing so the system promotes a faster evolution of guidance& navigational control algorithms, and the development of insect inspired sensor systems, ultimately working towards 'saving lives' in terrorist and environmental disaster situations.

VI. References

VI. References:

[1]. Jimonics Engineering Solutions, www.jimonics.com, Accessed Dec 2006

[2]. A Brief History of UAV's, http://www.list.ufl.edu/uav/UAVHstry.htm, Accessed Dec 2006

[3]. Srinivasan, M.V., Zhang, S.W., Lehrer, M., and Collett, T.S, "Honeybee Navigation En Route To The Goal: Visual Flight Control And Odometery", Larry Lipera, The Journal of Experimental Biology 199, 237–244 (1996), Printed in Great Britan, 2006

[4]. Melhuish, C. and Welsby, J., "Gradient Ascent with a group of Minimalist Real Robots: Implementing Secondary Swarming,", Proceedings of the IEEE International Conference on Systems, Man and Cybernetics, 2002

[5]. Delfly, http://www.delfly.nl , Accessed Dec 2006

[6]. E-puck, http://www.e-puck.org, Accessed Dec 2006

[7]. Khepera, http://www.k-team.com, Accessed Dec 2006

[8]. Blade Runner, Proxflyer, http://www.proxflyer.com/bl_meny.htm, Accessed Dec 2006

[9]. Photograph, Proxflyer – Blade Runner, Taken 25 Nov 2006

[10]. X-UFO, Firebox, http://www.firebox.com/?action=product&dir=firebox&pid=1024 , Accessed Dec 2006

[11]. Twister Bell-47, Model Flight, http://www.modelflight.com.au/pics/twister_bell_47g.jpg, Accessed March 2007

[12]. Mr. Kimio NAKAMURA's Coaxis Micro Helicopter, http://liaison.ms.u-tokyo.ac.jp/agusta/coaxis/nakamura.html, Accessed March 2007

[13]. Photograph, Twister Bell-47, Taken 25 Nov 2006

[14]. Schluter's Radio Controlled Helicopter Manual, Dieter Schluter, 1981

[15]. GFS UAV Project, JLN Labs, http://jlnlabs.imars.com/gfsuav/index.htm, Accessed Dec 2006

[16]. Coander Effect Test Bench, JLN Labs, http://jlnlabs.imars.com/gfsuav/index.htm, Accessed Dec 2006

[17]. Lipera, L., Colbourne, J.D., Tischler, M.B., Mansur, M.H., Rotkowitz, M.C. and Patangui, P., "The Micro Craft iSTAR Micro Air Vehicle Control System Design and Testing", American Helicopter Society 57th Annual forum, Washington, DC, May 9-11, 2001

[18]. Microdrones, GMBH, http://www.microdrones.com/, Accessed Dec 2006

[19]. Downloads, Videos, Microdrones, http://www.microdrones.com/, Accessed Dec 2006

[20]. Green, W.E. and Oh, P.Y., "Autonomous Hovering of a Fixed-Wing Micro Air Vehicle", Drexel Autonomous Systems Lab, Drexel University, Philadelphia, PA, May 2006

[21]. Samuel, P. and Gessow, A., "Design and Testing of a Rotary Wing MAV with an Active Structure for Stability and Control", Rotorcraft Center Department of Aerospace Engineering University of Maryland College Park, June 2005

[22]. Wu, M.H. and Schetky, L.M., "Industrial Applications For Shape Memory Alloys", Proceedings of the International Conference on Shape Memory and Super elastic Technologies, Pacific Grove, California, P.171-182 (2000).

[23]. Buysschaert, F., "Piezoelectric Actuators for Cyclic and Collective Control of UAV Helicopter Blades", Royal Military Academy, Civil and Materials Engineering Department Av. de la Renaissance 30, B-1000, Brussels, (Publish Date Unavailable)

[24]. Bohorquez, F. and Gessow, A., "Design, Analysis and Performance of a Rotary Wing MAV", Smart Structures Laboratory & Rotorcraft Center Department of Aerospace Engineering, University of Maryland College Park, MD 20742, (Publish Date Unavailable)

[25]. Mosquito Twin-tail - 130 grams, Proxflyer, www.proxflyer.com , Accessed Dec 2006

[26]. Venom Outback Rescue, Model Flight, http://www.modelflight.com.au/rc_model_helicopters/outback_rescue_helicopter.htm Accessed Dec 2006

[27]. Photograph, Venom Outback Rescue, Taken 20 Nov 2006

[28]. Leishman, J.G., "Principles of Helicopter Aerodynamics", Cambridge Aerospace Series, Book Published 2006, Cambridge University Press, Pg 101, ISBN 0521858607

[29]. Simon, D., “Kalman Filtering”, Embedded Systems Programming Magazine, Pg 72, June 2001

[30]. Park, S. and How, J., “Examples of Estimation Filters from Recent Aircraft Projects at MIT”, November 2004

[31]. nIMU & MAG3, Memsense, http://www.memsense.com/,Accessed Nov 2006

[32]. MMA1260D & MMA2260D Datasheets, Accelerometer, Freescale www.freescale.com, Accessed Nov 2006

[33]. HMC1022 Datasheet, Honeywell, www.honeywell.com, Accessed Nov 2006

[34]. Standard Atmosphere Calculator, http://www.digitaldutch.com/atmoscalc/, Accessed Nov 2006

[35]. Ideal Gas Law Equation, http://www.ajdesigner.com/idealgas/index.php , Accessed Nov 2006

[36]. Euler Angles, Tensor Conventions, http://anorganik.uni-tuebingen.de/klaus/nmr/conventions/euler/euler.html, Accessed Nov 2006

[37]. PID Controller, PID Without a PhD, http://www.embedded.com/2000/0010/0010feat3.htm, Accessed Nov 2006

[38]. LQR Controller, Linear Quadratic Regulator, http://en.wikipedia.org/wiki/Linear-quadratic_regulator, Accessed Nov 2006

[39]. NN Controller, Neural Network, http://en.wikipedia.org/wiki/Neural_network, Accessed Nov 2006

[40]. MP Controller, Model Predictive Control, http://en.wikipedia.org/wiki/Model_predictive_control, Accessed Nov 2006

[41]. AXI Brushless Motor, Model Flight, http://www.modelflight.com.au/axi.htm, Accessed Nov 2006

[42]. Sabahoceanic, Lithium, http://www.sabahoceanic.com/images/603870H.jpg, Accessed Nov 2006

[43]. PIC18F452 Datasheet, www.microchip.com, Accessed Nov 2006

[44]. ATMEGA162 Datasheet, www.atmel.com, Accessed Nov 2006

[45]. SCM-18, Servo Controller Module, Jimonics Engineering Solutions, www.jimonics.com, Accessed Nov 2006

[46]. Skyborne 14, SJ Propo, http://www.hstore.com.au/ , Accessed Nov 2006

[47]. 9-Xtend OEM, Maxstream, www.maxstream.net , Accessed Nov 2006

[48]. Xbee Pro, Maxstream, www.maxstream.net , Accessed Nov 2006

[49]. Wiport, Lantronix, www.lantronix.com, Accessed Nov 2006

[50]. Autopilot, http://sourceforge.net/project/showfiles.php?group_id=36164, Accessed Nov 2006

[51]. JR XF631Remote, http://www.greatmodeldeals.com/buy/pics/jrxf631.jpg, Accessed Nov 2006

[52]. Adaptation, Berkeley http://evolution.berkeley.edu/evosite/evo101/images/bat_echolocation_225.gif, Accessed March 2007

[53]. Echolocation: Through Sea Water and the mathematical concepts that detail this problem, Mark Young and Mary Adekola http://ace.acadiau.ca/math/karsten/Projectwebpages/echolocationpic.gif, Accessed March 2007

[54]. ISPAVRU1 Programmer, ERE CO LTD http://www.ere.co.th , Accessed March 2007

[55]. The LV-MaxSonar®-EZ1™ High Performance Ultrasonic Range Finder, MaxBotix® http://www.maxbotix.com/, Accessed March 2007

[56]. C Compiler, Code Vision http://www.hpinfotech.ro/html/cvavr.htm, Accessed March 2007

VII. Appendix:

1.0 Sensor Schematics

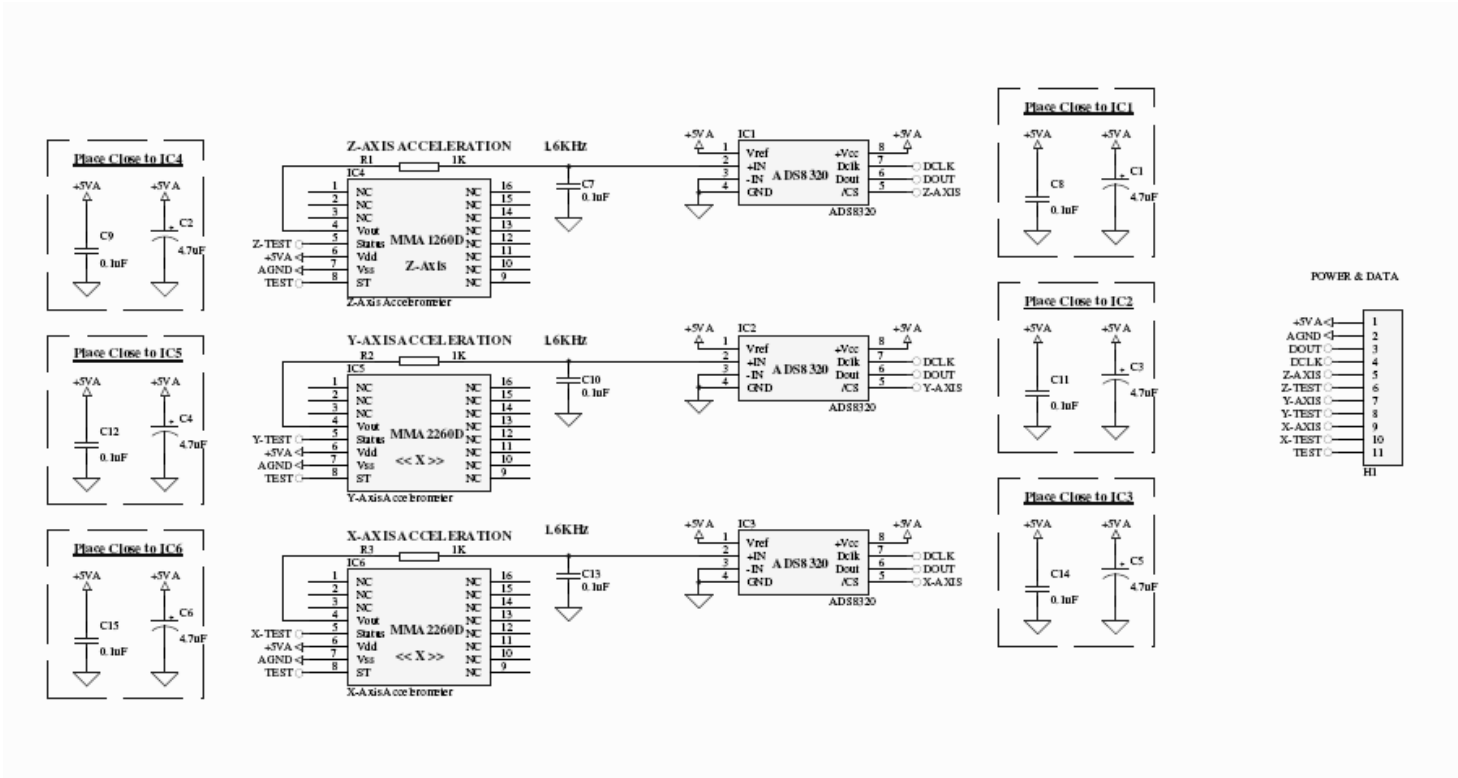

Figure 89: "G-Cell" 3D Accelerometer Schematic

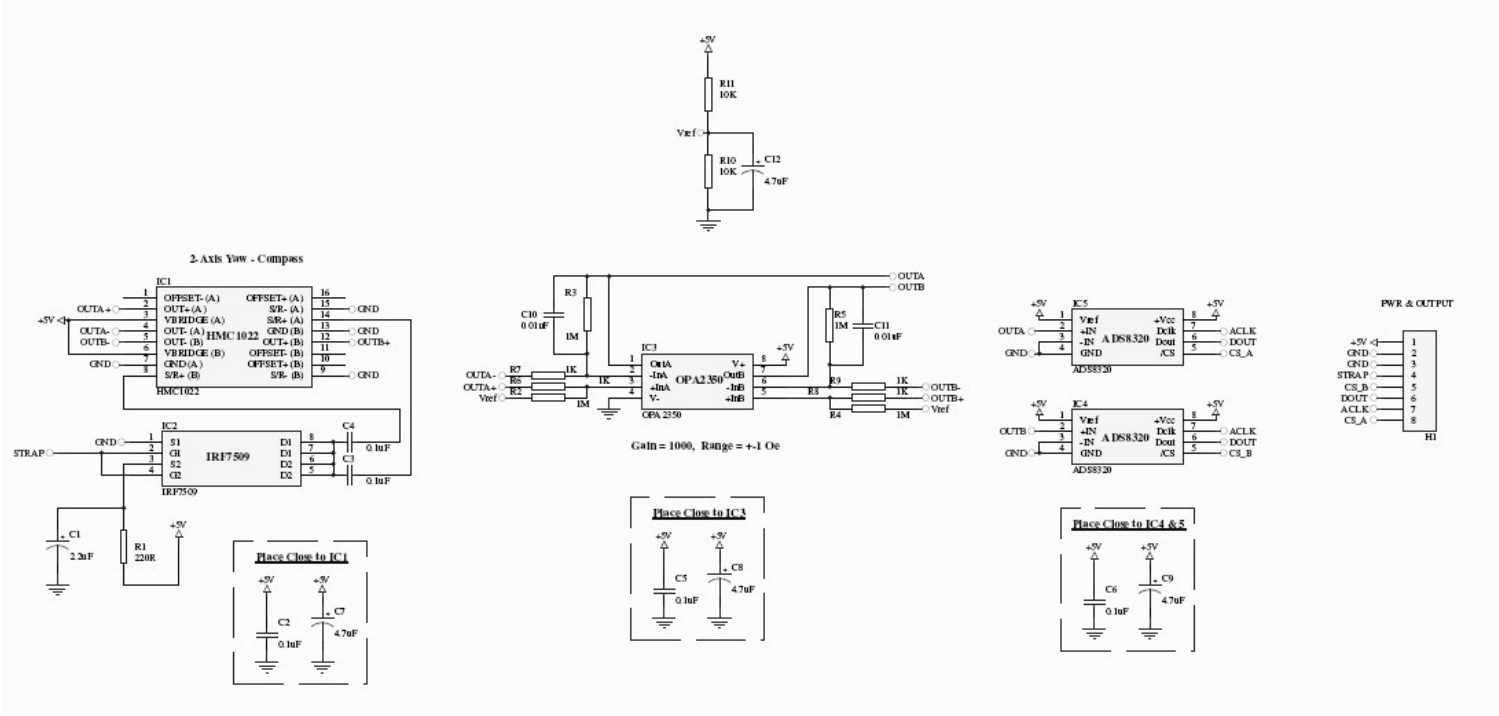

Figure 90: "Star-2" 2-Axis Magnetometer Schematic

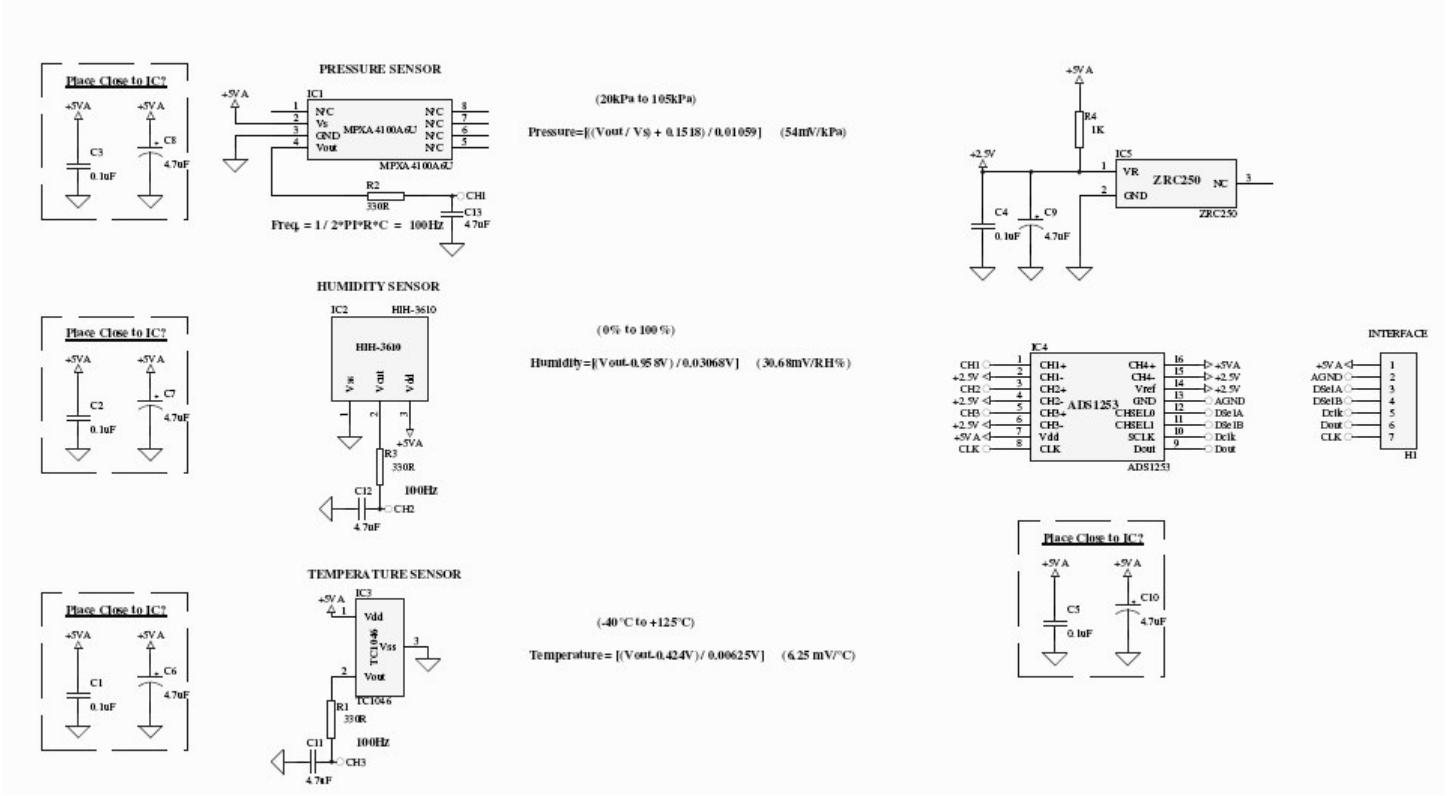

Figure 91: "Sky-3" Pressure Altitude Schematic

2.0 “The MicroBrain” Schematic

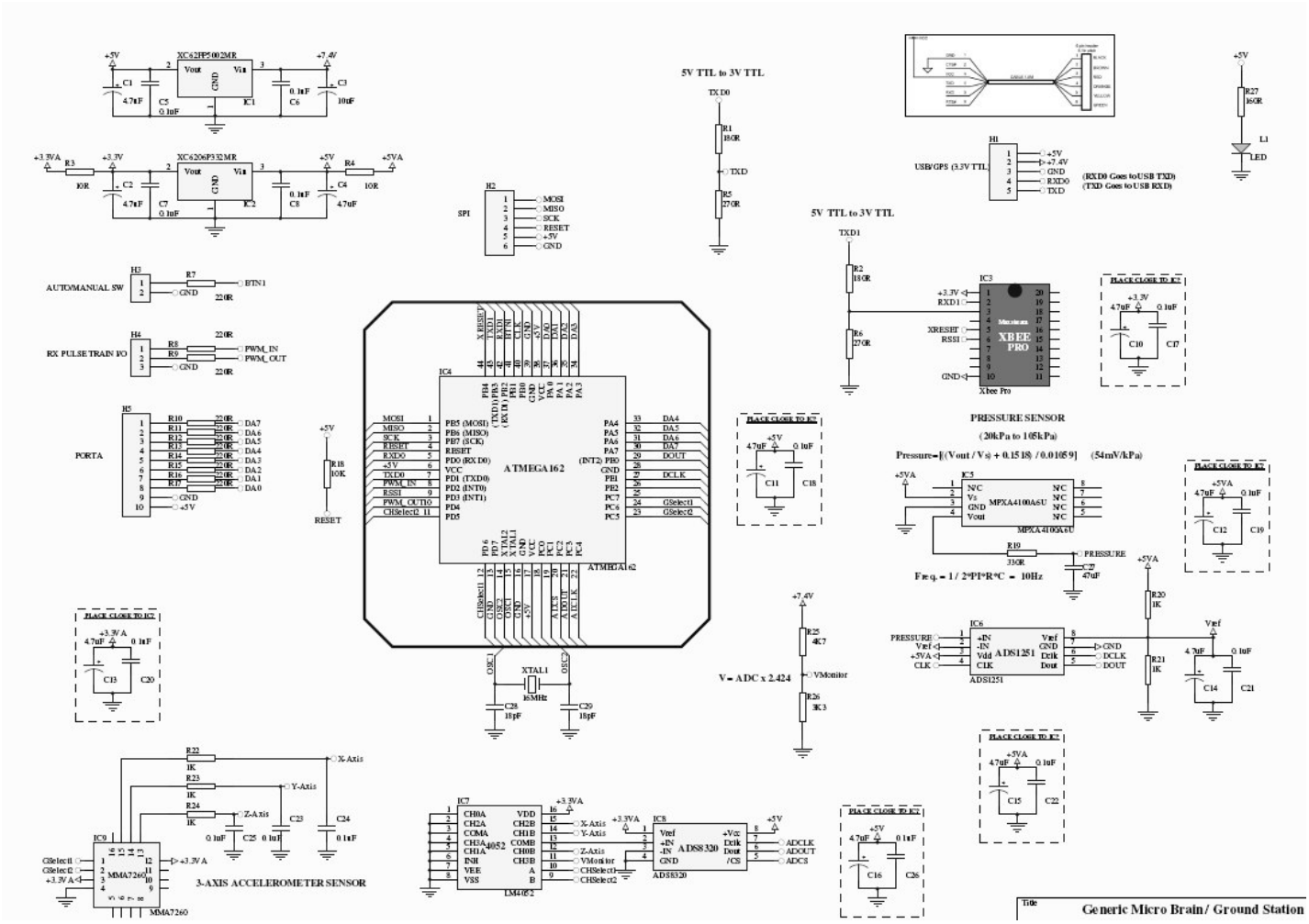

Figure 92: "The MicroBrain" Schematic